MCB
Journals.ASM.org

A Novel Histone Deacetylase Complex in the Control of Transcription and Genome Stability

Nicola Zilio,[a] Sandra Codlin,[b] Ajay A. Vashisht,[d] Danny A. Bitton,[b] Steven R. Head,[c] James A. Wohlschlegel,[d] Jürg Bähler,[b] Michael N. Boddy[a]

Department of Cell and Molecular Biology, The Scripps Research Institute, La Jolla, California, USA[a]; University College London, Department of Genetics, Evolution & Environment, and UCL Cancer Institute, London, United Kingdom[b]; Next Generation Sequencing Core, The Scripps Research Institute, La Jolla, California, USA[c]; Department of Biological Chemistry, David Geffen School of Medicine, University of California, Los Angeles, California, USA[d]

The acetylation state of histones, controlled by histone acetyltransferases (HATs) and deacetylases (HDACs), profoundly affects DNA transcription and repair by modulating chromatin accessibility to the cellular machinery. The *Schizosaccharomyces pombe* HDAC Clr6 (human HDAC1) binds to different sets of proteins that define functionally distinct complexes: I, I′, and II. Here, we determine the composition, architecture, and functions of a new Clr6 HDAC complex, I′′, delineated by the novel proteins Nts1, Mug165, and Png3. Deletion of *nts1* causes increased sensitivity to genotoxins and deregulated expression of *Tf2* elements, long noncoding RNA, and subtelomeric and stress-related genes. Similar, but more pervasive, phenotypes are observed upon Clr6 inactivation, supporting the designation of complex I′′ as a mediator of a key subset of Clr6 functions. We also reveal that with the exception of *Tf2* elements, the genome-wide loading sites and loci regulated by Clr6 I″ do not correlate. Instead, Nts1 loads at genes that are expressed in midmeiosis, following oxidative stress, or are periodically expressed. Collective data suggest that Clr6 I′′ has (i) indirect effects on gene expression, conceivably by mediating higher-order chromatin organization of subtelomeres and *Tf2* elements, and (ii) direct effects on the transcription of specific genes in response to certain cellular or environmental stimuli.

Epigenetic mechanisms, such as the covalent modification of histones with certain chemical groups or entire proteins, exert critical control over the structure and function of genomes (1). A major and highly regulated type of histone modification is the acetylation of lysine residues. Histone acetylation is controlled by the concerted actions of histone acetyltransferases (HATs) and histone deacetylases (HDACs) (2, 3).

HDACs fall into three main classes, I through III, based on their phylogenetic relationship to the prototypical budding yeast HDACs, their subcellular localization, and their enzymatic activities. Like humans, the fission yeast *Schizosaccharomyces pombe* possesses members of all three classes: Clr6 (class I, orthologue of budding yeast Rpd3 and human HDAC1/2), Clr3 (class II, part of SHREC and orthologous to budding yeast Hda1), and Sir2/Hst2/Hst4 (class III). Clr6 is an essential gene; compromising its function leads to increased bulk histone acetylation levels with pleiotropic consequences: the upregulation of RNA from protein-coding, subtelomeric, long noncoding RNA genes and repetitive elements, abnormal chromosome structure, and increased sensitivity toward DNA-damaging agents (4–6).

Like budding yeast Rpd3, Clr6 exists in two complexes that regulate euchromatin and heterochromatin in similar manners (5). Complex I includes the essential proteins Sds3, Prw1, PstI/3, Rxt2/3, and Laf1/2. It deacetylates somewhat preferentially gene promoters, thus regulating sense transcription of protein-coding genes. It also controls sense transcription of the *dg/dh* repeats that are found at all major heterochromatic sites in fission yeast (7). Complex II, which includes the nonessential proteins Pst2, Alp13, and Cph1/2, preferentially deacetylates intragenic regions and represses antisense transcription of protein-coding genes and that of *dg/dh* repeats. Thus, compromising the integrity of complex II leads to a pervasive increase in the levels of antisense RNAs, which are processed by the exosome. Complex II deficiency also causes genotoxin sensitivity, likely through the misregulation of chromatin structure.

Besides *dg/dh* repeats, Clr6 also controls other repetitive elements, such as the *Tf2* retrotransposons. Cells carrying the temperature-sensitive allele *clr6-1* exhibit increased levels of RNA from both the *Tf2* long terminal repeat (LTRs) and the intervening retrotransposase open reading frame (ORF), which are normally very low (8, 9). Similar transcriptional defects arise in cells lacking the class II HDAC Clr3, the three partially redundant fission yeast CENP-B-like proteins Abp1, Cbh1, and Cbh2, or the histone chaperone complex HIRA (Hip1, -3, or -4, Slm9, and ClaI), indicating functional overlap of these proteins at retrotransposons (9–12). Indeed, the recruitment of Clr6 to Tf2 retrotransposons is mediated in part by Abp1, which binds a 10-nucleotide (nt) AT-rich motif found in the *Tf2* LTRs.

Loss of function of Abp1, Cbh1, Cbh2, Clr6, and Clr3, as well as the class III HDACs Hst2 and Hst4, also compromises the integrity of *Tf* bodies, which are subnuclear structures into which *Tf2* elements cluster (8, 12). *Tf* bodies are proposed to keep retrotransposons in a silenced state, thus helping maintain genome stability by preventing uncontrolled retrotransposition. The histone methyltransferase Set1 suppresses transcription of *Tf2* elements and also maintains the integrity of *Tf* bodies (12). Interestingly, although its functions are largely overlapping with

Received 16 April 2014 Returned for modification 12 May 2014
Accepted 30 June 2014
Published ahead of print 7 July 2014
Address correspondence to Michael N. Boddy, nboddy@scripps.edu.
Copyright © 2014, American Society for Microbiology. All Rights Reserved.
doi:10.1128/MCB.00519-14

TABLE 1 List of the yeast strains used in this study

Strain	Genotype[a]	Source or reference
NB511I	*nse3-1-myc$_{13}$:kanMX6 h$^-$*	52
NB526	*nse1-1-myc$_{13}$:kanMX6 h$^+$*	52
NB527	*nse2-1-myc$_{13}$:kanMX6 h$^+$*	52
NB835	*nse6::kanMX6 h$^+$*	28
NB895	*nse5::kanMX6 h$^-$*	28
NB780	*h$^+$*	
NB781	*h$^-$*	
NB1533	*nse4-3-3HA:hphMX6 h$^-$*	
NB3679	pREP(*adh*):*ura4$^+$* integrated at *ars1 h$^-$*	
NB4066	*nts1-eGFP:hphMX6 h$^+$*	
NB4969	*nts1-eGFP:hphMX6 cdc25-22*	
NB4091	*nts1::hphMX6 h$^+$*	
NB4541	*clr6-myc$_{13}$:hphMX6 h$^-$*	
NB4607	*clr6-myc$_{13}$:hphMX6 nts1-TAP:kanMX6*	
NB4608	*clr6-myc$_{13}$:hphMX6 mug165-TAP:kanMX6*	
NB4609	*clr6-myc$_{13}$:hphMX6 png3-TAP:kanMX6*	
NB4610	*clr6-myc$_{13}$:hphMX6 fkh2-TAP:kanMX6*	
NB4542	*sds3-myc$_{13}$:hphMX6 h$^-$*	
NB4611	*sds3-myc$_{13}$:hphMX6 nts1-TAP:kanMX6*	
NB4612	*sds3-myc$_{13}$:hphMX6 mug165-TAP:kanMX6*	
NB4613	*sds3-myc$_{13}$:hphMX6 png3-TAP:kanMX6*	
NB4614	*sds3-myc$_{13}$:hphMX6 fkh2-TAP:kanMX6*	
NB4093	*nts1-myc$_{13}$:hphMX6 h$^+$*	
NB4619	*nts1-myc$_{13}$:hphMX6 fkh2-TAP:kanMX6*	
NB4615	*nts1-myc$_{13}$:hphMX6 clr6-TAP:kanMX6*	
NB4617	*nts1-myc$_{13}$:hphMX6 mug165-TAP:kanMX6*	
NB4616	*nts1-myc$_{13}$:hphMX6 sds3-TAP:kanMX6*	
NB4618	*nts1-myc$_{13}$:hphMX6 png3-TAP:kanMX6*	
NB4543	*mug165-myc$_{13}$:hphMX6 h$^-$*	
NB4623	*mug165-myc$_{13}$:hphMX6 fkh2-TAP:kanMX6*	
NB4621	*mug165-myc$_{13}$:hphMX6 nts1-TAP:kanMX6*	
NB4573	*mug165-myc$_{13}$:hphMX6 clr6-TAP:kanMX6*	
NB4574	*mug165-myc$_{13}$:hphMX6 sds3-TAP:kanMX6*	
NB4622	*mug165-myc$_{13}$:hphMX6 png3-TAP:kanMX6*	
NB4605	*png3-myc$_{13}$:hphMX6 h$^-$*	
NB4649	*png3-myc$_{13}$:hphMX6 fkh2-TAP:kanMX6*	
NB4647	*png3-myc$_{13}$:hphMX6 nts1-TAP:kanMX6*	
NB4645	*png3-myc$_{13}$:hphMX6 clr6-TAP:kanMX6*	
NB4648	*png3-myc$_{13}$:hphMX6 mug165-TAP:kanMX6*	
NB4646	*png3-myc$_{13}$:hphMX6 sds3-TAP:kanMX6*	
NB4606	*fkh2-myc$_{13}$:hphMX6 h$^-$*	
NB4652	*fkh2-myc$_{13}$:hphMX6 nts1-TAP:kanMX6*	
NB4650	*fkh2-myc$_{13}$:hphMX6 clr6-TAP:kanMX6*	
NB4653	*fkh2-myc$_{13}$:hphMX6 mug165-TAP:kanMX6*	
NB4651	*fkh2-myc$_{13}$:hphMX6 sds3-TAP:kanMX6*	
NB4708	*fkh2-myc$_{13}$:hphMX6 png3-TAP:kanMX6*	
NB4869	*png2-myc$_{13}$:hphMX6 h$^-$*	
NB4876	*png2-myc$_{13}$:hphMX6 nts1-TAP:kanMX6*	
NB4875	*png2-myc$_{13}$:hphMX6 clr6-TAP:kanMX6*	
NB4900	*alp13-myc$_{13}$:hphMX6 h$^-$*	
NB4915	*alp13-myc$_{13}$:hphMX6 nts1-TAP:kanMX6*	
NB4614	*alp13-myc$_{13}$:hphMX6 clr6-TAP:kanMX6*	
NB4724	*mug165-myc$_{13}$:hphMX6 sds3-TAP:kanMX6 nts1::hphMX6*	
NB4725	*mug165-myc$_{13}$:hphMX6 sds3-TAP:kanMX6 png3::hphMX6*	
NB4726	*png3-myc$_{13}$:hphMX6 mug165-TAP:kanMX6 nts1::hphMX6*	
NB4723	*mug165-myc$_{13}$:hphMX6 nts1-TAP:kanMX6 png3::hphMX6*	
NB4720	*nts1-myc$_{13}$:hphMX6 sds3-TAP:kanMX6 mug165::hphMX6*	
NB4721	*nts1-myc$_{13}$:hphMX6 sds3-TAP:kanMX6 png3::hphMX6*	
NB4727	*png3-myc$_{13}$:hphMX6 sds3-TAP:kanMX6 nts1:hphMX6*	
NB4728	*png3-myc$_{13}$:hphMX6 sds3-TAP:kanMX6 mug165:hphMX6*	
NB4722	*nts1-myc$_{13}$:hphMX6 png3-TAP:kanMX6 mug165:hphMX6*	
NB4545	*mug165::hphMX6*	
NB4748	*png3::natMX6*	
NB4757	*nse6::kanMX6* pREP(*adh*)-*nts1$^+$*:*ura4$^+$* integrated at *ars1*	
NB4759	*nts1::hphMX6 mug165::natMX6*	
NB4760	*nts1::hphMX6 png3::natMX6*	
NB4762	*mug165::hphMX6 png3::natMX6*	
NB4770	pREP(*adh*)-*nts1$^+$*:*ura4$^+$* integrated at *ars1 h$^-$*	
NB4777	*nse6::kanMX6* pREP(*adh*):*ura4$^+$* integrated at *ars1 h$^-$*	
NB4828	*nts1::natMX6 mug165::hphMX6 png3::natMX6*	
NB4718	*clr6-1*	Derived from reference 4
NB5313	*clr6-1 nts1::natMX6*	
NB5130	*nts1-FLAG$_3$::kanMX6 SPNCRNA.276/30::hphMX6* pNZ84(pJK148-based):*leu1$^+$*	
NB5132	*nts1-FLAG$_3$::kanMX6 SPNCRNA.276/30::hphMX6* pNZ86(pJK148-based):*leu1$^+$*	
NB5133	*nts1-FLAG$_3$::kanMX6 SPNCRNA.276/30::hphMX6* pNZ87(pJK148-based):*leu1$^+$*	
NB4228	*nts1-FLAG$_3$::kanMX6*	
NB5053	*nts1-FLAG$_3$::kanMX6*	
NB1367	*nse2-FLAG$_3$::kanMX6*	
NB5090	*sds3-FLAG$_3$::kanMX6*	
NB5091	*sds3-FLAG$_3$::kanMX6 nts1::natMX6*	
NB5094	*sds3-FLAG$_3$::kanMX6 nts1::natMX6 mug165::hphMX6 png3::natMX6*	
NB4849	*clr4::natMX6 otr1*(SphI)::*ura4$^+$ ade6-210*	53
NB5276	*tf2-2*(LTR-*lacZ*):*ura4$^+$*	Derived from reference 11
NB5280	*tf2-2*(LTR-*lacZ*):*ura4$^+$ nts1::natMX6*	
NB5277	*tf2-3*(LTR-*lacZ*):*ura4$^+$*	Derived from reference 11
NB5281	*tf2-3*(LTR-*lacZ*):*ura4$^+$ nts1::natMX6*	
NB5278	*tf2-10*(LTR-*lacZ*):*ura4$^+$*	Derived from reference 11
NB5282	*tf2-10*(LTR-*lacZ*):*ura4$^+$ nts1::natMX6*	
NB5279	*tf2-11*(LTR-*lacZ*):*ura4$^+$*	Derived from reference 11
NB5283	*tf2-11*(LTR-*lacZ*):*ura4$^+$ nts1::natMX6*	

[a] All strains are of *ura4-D18 leu1-32* background genotype, unless otherwise stated. Double colons represent knockouts; single colons represent tagging.

Abp1 with respect to silencing of *Tf2* element sense transcription, Abp1 and Set1 control antisense transcription through different mechanisms (12).

In a screen for genes whose overexpression can suppress the phenotypes caused by structural maintenance of chromosome complex Smc5-Smc6 deficiency, we identified a previously uncharacterized gene that we called *nts1*. Here, we demonstrate that Nts1 is a nuclear protein, which together with two other previously uncharacterized proteins, Mug165 and Png3, maintains genome stability. Moreover, Nts1, Mug165, and Png3 define a new variant of the Clr6 complex I that controls the expression of *Tf2* elements and subtelomeric, noncoding RNA (ncRNA), and stress-related genes.

MATERIALS AND METHODS

Strains and growth conditions. Standard fission yeast culture and handling were used as described in reference 13. All strains are of genotype *ura4-D18 leu1-32* unless otherwise stated. Table 1 contains a list of the strains used to prepare this report.

Spot assay. Yeast was propagated in yeast extract with supplements (YES medium) at 30°C to logarithmic phase (optical density at 600 nm [OD_{600}] of 0.6 to 0.8), spotted on YES agar supplemented with the relevant drug in 5-fold dilutions from a starting OD_{600} of 0.5, and then incubated at 30°C for 2 to 3 days. A Stratalinker-1800 cross-linker instrument (Stratagene, La Jolla, CA) was used to irradiate plates with UV light at 365 nm.

Fluorescence microscopy. Images of live cells were captured on an Eclipse E800 microscope (Nikon Metrology, Brighton, MI), and images were acquired with a Quantix camera (Photometrics, Tucson, AZ).

Preparation of whole-cell extracts and Western blotting. Denatured whole-cell extracts were prepared as described in reference 14. A total of 50 μg of protein was resolved on 4 to 20% Tris-glycine gels (Expedeon, San Diego, CA) and transferred to a nitrocellulose membrane with an iBlot dry blotting transfer system (Life Technologies, Carlsbad, CA). The membrane was blocked in 5% (wt/vol) nonfat milk in Tris-buffered saline solution with 0.1% (vol/vol) Tween 20 before being blotted first with antibodies against the FLAG epitope (M2; Sigma-Aldrich, Saint Louis, MO) and then an IRDye-conjugated secondary antibody (Li-Cor, Lincoln, NE). The membrane was imaged on an ODYSSEY scanner (Li-Cor).

Purification of $FLAG_3$-Nts1-TAP. For proteomic analysis of immunoprecipitated Nts1, exponentially growing cells (8,000 OD_{600} units) were washed, resuspended with 0.25 cell pellet volumes of 20 mM HEPES (pH 7.6) and 50 mM NaCl, flash-frozen as "popcorn," ground in a pestle grinder (Retsch, Newtown, PA) until >75% had lysed, and resuspended in 90 ml of 20 mM HEPES (pH 7.6), 150 mM NaCl, 1 mM EDTA, 0.8% (vol/vol) NP-40, 10% (vol/vol) glycerol, 2 mM phenylmethylsulfonyl fluoride (PMSF), and 1× Complete protease inhibitors (Roche, Indianapolis, IN). The lysate was cleared by centrifugation at 20,000 × *g* for 30 min at 4°C, adjusted to 100 ml at 15 mg ml^{-1} of total protein, and incubated with 0.5 ml of preequilibrated IgG resin (GE Healthcare Life Sciences) overnight at 4°C with rotation. Next, the resin was washed three times with 2 ml of the lysis solution described above without protease inhibitors, once with 50% of the same solution and 50% of 20 mM HEPES (pH 7.6), 150 mM NaCl, 0.1% (vol/vol) NP-40, and 1 mM EDTA, and once with 100% of the latter solution. The IgG resin was resuspended with 0.75 ml of the latter solution supplemented with 0.75 mM dithiothreitol (DTT) and 500 U of tobacco etch virus (TEV) protease (Eton Biosciences, San Diego, CA) and incubated at room temperature for 4 h with rotation. The resin was washed three times with 0.5 ml of the same solution used for proteolysis, which was combined with the eluate, supplemented with 0.25 ml of preequilibrated anti-FLAG resin (M2; Sigma-Aldrich), and incubated overnight at 4°C with rotation. The anti-FLAG resin was washed three times with 1 ml of the same solution used for binding to the anti-FLAG resin and eluted five times for 20 min with 0.25 ml of the same solution supplemented with 0.5 μg ml^{-1} 3× FLAG peptide (F4799; Sigma-Aldrich). The eluted proteins were trichloroacetic acid (TCA) precipitated, washed in ice-cold acetone, and subjected to mass spectrometry.

For the large-scale chromatin immunoprecipitation (ChIP) assay, 700 OD_{600} units of cells were processed in 14 equal aliquots as per the ChIP assay described below to yield 10 ml of whole-cell extract at 15 mg ml^{-1} of total protein. This lysate was supplemented with 200 μl of IgG resin and processed as described above, with the only difference being that the volume of the washes was halved. The anti-FLAG resin was washed as per the ChIP assay described below, using a volume of 10 ml for each wash, and eluted twice with 0.5 ml of 10 mM Tris (pH 8), 1 mM EDTA, and 1% (vol/vol) SDS for 15 min at 70°C. The eluted DNA was de-cross-linked and recovered as per the ChIP protocol described below.

Mass spectrometry. Protein samples were denatured, reduced, alkylated, and digested with trypsin (15, 16). The digested proteins were loaded onto a triphasic MudPIT column (3 cm of reversed-phase resin followed by 3 cm of strong cation-exchange resin and ending with 10 cm of reversed-phase resin) that was connected in line with a 1200 quaternary high-performance liquid chromatography (HPLC) pump (Agilent Technologies, Santa Clara, CA) and electrosprayed directly into an LTQ Orbitrap XL mass spectrometer (Thermo Scientific, Waltham, MA) using a 10-step MudPIT method (15, 16). Tandem mass spectrometry (MS/MS) spectra were extracted using RawXtract and searched with Sequest against the *Schizosaccharomyces pombe* UniProt database (17). Sequest results were assembled and filtered using DTASelect (18, 19). Peptide identifications were filtered using a false-positive rate of 0.05 as estimated using a decoy database approach (20).

Coimmunoprecipitation. Whole-cell extracts for coimmunoprecipitation studies were prepared from 50 OD_{600} units of cells by bead beating and centrifugation as described in reference 14 in 20 mM HEPES (pH 7.6), 150 mM NaCl, 1 mM EDTA, 0.5% (vol/vol) NP-40, 10% (vol/vol) glycerol, 1× Complete protease inhibitor cocktail, and 2 mM PMSF. The lysates were adjusted to 1 ml at 2 μg μl^{-1} total protein and incubated with 20 μl of IgG-Sepharose 6 resin (GE Healthcare Life Sciences, Pittsburgh, PA) for 2 h at 4°C with rotation. The beads were washed 4 times in 0.5 ml of the lysis buffer described above, without protease inhibitors, and eluted in 40 μl of 1.5× NuPAGE lithium dodecyl sulfate (LDS) sample buffer (Life Technologies) supplemented with 100 mM DTT at 95°C for 5 min. For Western blotting, we loaded 20 μg of total protein for the input samples and 20% (vol/vol) of the immunoprecipitate eluate. Blotting of TAP and Myc tags was done with the peroxidase-antiperoxidase complex (PAP antibody; Sigma-Aldrich) and an anti-Myc antibody (9E10; in house), respectively.

RNA extraction, microarray analysis, and reverse transcription-quantitative PCR (RT-qPCR). Total RNA was extracted from ~5 OD_{600} units of exponentially growing cells (three independently harvested batches) by the hot-phenol method as described in reference 21. Microarray analysis was carried out as described in reference 22 using a custom-designed 44K microarray chip (Agilent Technologies), with the following modifications. For labeling, Alexa Fluor 555- or 647-labeled cDNA was produced from the RNA with a Superscript direct cDNA labeling system (Life Technologies) and Alexa Fluor dUTP label mix. The cDNA was purified using a PureLink PCR purification system (Life Technologies). The cDNA was hybridized to the array using a gene expression hybridization kit (Agilent Technologies). Following hybridization for at least 17 h, the chip was washed using a gene expression wash buffer kit (Agilent Technologies). The data were normalized using a customized R script which combines local normalization (22) and global normalization ("normalizeWithinArrays" function from Limma package using the LOESS method). Enrichments were determined by using a test in GeneSpring (Agilent Technologies) based on the hypergeometric distribution.

For RT-qPCR, 15 μg of total RNA was incubated with DNase I (3 U; NEB, Ipswich, MA) in a 100-μl reaction mixture as described by the manufacturer. DNase-treated RNA was purified with the RNeasy Plus minikit (Qiagen, Germantown, MD) by following the manufacturer's instructions. A total of 1 μg of DNase-treated total RNA was reverse transcribed using the EasyScript cDNA synthesis kit (Lamda Biotech, Ballwin, MO) in a total volume of 20 μl with 2 μM dT_{16}, by following the manufacturer's instruction. The completed reactions were diluted 10-fold, and 5 μl of these dilutions was used as the template in 20-μl qPCR mixtures using the EvaGreen Mastermix-S (Lamda Biotech), as described by the manufacturer.

Statistical analysis of clustering of *nts1*-regulated genes. To determine whether *nts1*-regulated genes cluster at specific chromosomal locations, we sorted all nucleus-encoded fission yeast genes by their chromosomal locations (6,984; Ensembl v.13) (23) and used Fisher's exact test to measure the degree and significance of the overlap between a sliding window of 100 genes and *nts1*-regulated genes. *P* values were corrected for multiple testing using the Bonferroni correction ("p.adjust" in R, http://www.R-project.org).

We used "phyper" in R to calculate the significance of overlap between *nts1*-regulated genes and those genes that directly overlap, or are within 500 bp of, *Tf2* LTRs or solo LTRs. *P* values represent the probability of observing the same number of overlaps, or more, by chance, assuming a hypergeometric distribution. We also evaluated the number of gene-LTR overlaps that would occur by chance. We randomly selected a set of genes from all nucleus-encoded fission yeast genes and measured the degree of overlap with those genes that directly intersect with, or are within 500 bp of, *Tf2* LTRs or their remnants. This step was repeated 1,000 times (permutations) for each list of *nts1*-regulated genes. These random gene sets were equal in size to their corresponding lists of *nts1*-regulated genes.

ChIP and qPCR. Cells (45 to 50 OD_{600} units) in 50 ml of growth medium were fixed in 1% (wt/vol) formaldehyde for 25 min at room temperature. The reaction was stopped by adding 2.6 ml of 2.5 M glycine. After the cells were extensively washed in Tris-buffered saline solution, they were lysed by bead beating as described in reference 14 in 0.5 ml of 50 mM HEPES (pH 7.6), 140 mM NaCl, 1 mM EDTA, 0.1% (vol/vol) Triton X-100, 1 mM PMSF, and 1× Complete protease inhibitor cocktail. Following the addition of Triton X-100 to 1% (vol/vol), chromatin was sheared by sonication in a Misonix Sonicator 3000 (Farmingdale, NY; 15 cycles of 30 s on at maximum intensity and 1 min off). The lysates were cleared by centrifugation and adjusted to 1 ml at 5 μg μl^{-1} or 2.5 μg μl^{-1} total protein, as determined by the Bradford assay, for immunoprecipitation against the FLAG tag or H3K9ac, respectively. After being precleared with 10 μl of preequilibrated bovine serum albumin (BSA)-blocked pro-

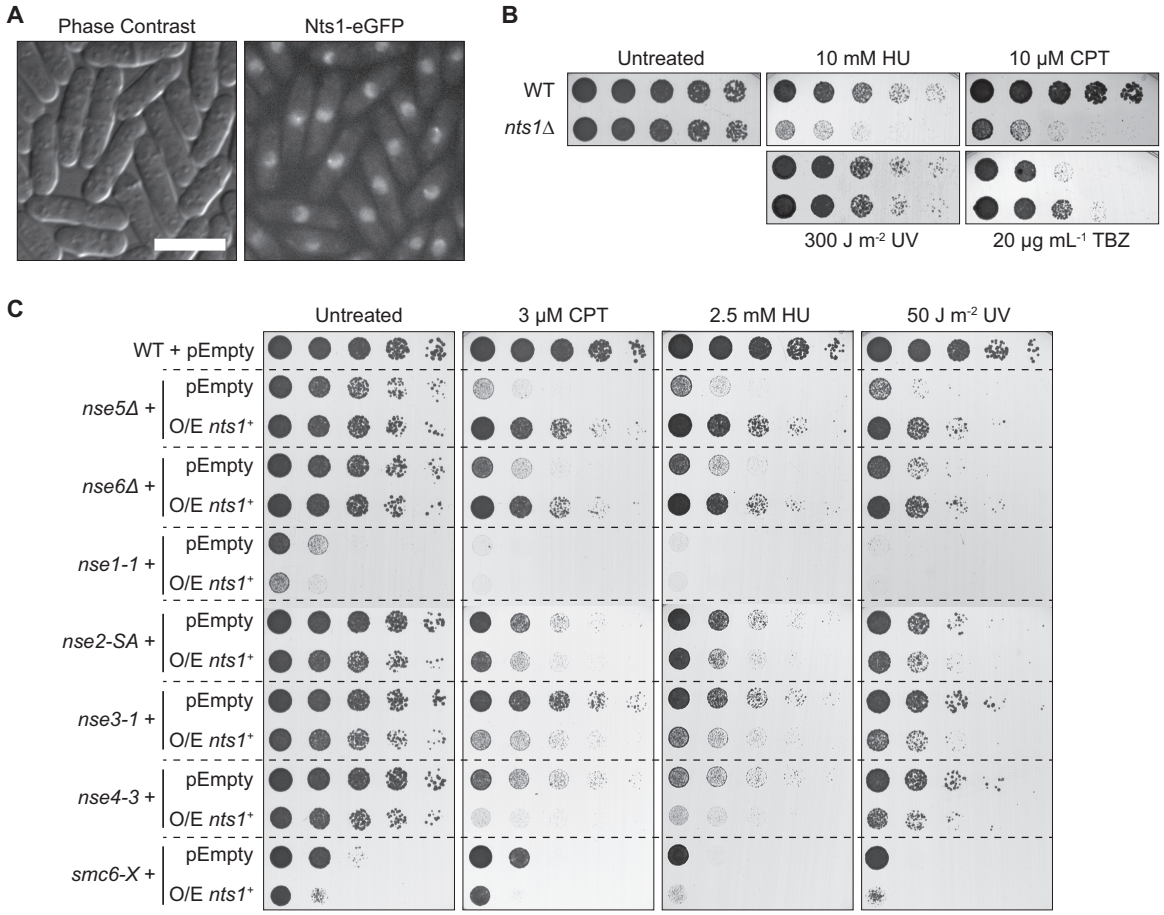

FIG 1 Nts1 is a nuclear protein that plays a role in genome stability. (A) Cells producing Nts1-enhanced green fluorescent protein (eGFP) were imaged by live fluorescence microscopy. The length of the bar equals 10 μm. (B and C) The noted strains were serially diluted onto rich medium (B) or Edinburgh minimal medium (C) in the presence of the indicated drugs and grown at 30°C. pEmpty, pREP2; O/E *nts1*$^+$, pREP4-*nts1*$^+$ (*nts1*$^+$ overexpression).

tein G MagBeads (GenScript, Piscataway, NJ) for 1 h at 4°C with rotation, the lysates were supplemented with either an anti-FLAG antibody (M2, 10 μg; Sigma-Aldrich) or anti-H3K9ac serum (number 39137, 4 μl; Active-Motif, Carlsbad, CA). After 2 h at 4°C with rotation, 10 μl of preequilibrated BSA-blocked protein G MagBeads was added to the samples and incubated for one more hour at 4°C with rotation. Next, the beads were washed three times for 10 min with 1 ml of 50 mM HEPES (pH 7.6), 140 mM NaCl, 1 mM EDTA, 1% (vol/vol) Triton X-100, and 0.1% (vol/vol) sodium deoxycholate, twice more in the same buffer but containing 500 mM NaCl, twice in 10 mM Tris-HCl (pH 8), 250 mM LiCl, 1 mM EDTA, 0.5% (vol/vol) NP-40, and 0.5% (vol/vol) sodium deoxycholate, and once in Tris-EDTA solution. DNA was eluted from the MagBeads with 150 μl of 10 mM Tris (pH 8), 1 mM EDTA, and 1% (vol/vol) SDS for 15 min at 70°C. De-cross-linking was performed overnight at 65°C. DNA was purified with Qiagen's PCR purification kit, eluted in 50 μl of water, and diluted 5-fold. A total of 5 μl of each of these samples was used as the template in 20-μl qPCR mixtures by using the EvaGreen Mastermix-S (Lamda Biotech), as described by the manufacturer.

Deep sequencing. Libraries from the Nts1 input and ChIP DNA samples were prepared by the nucleic acid core of The Scripps Research Institute and sequenced on a HiSeq instrument (Illumina, San Diego, CA) by following the manufacturer's instruction. The raw data sets were analyzed as follows: removal of the first 6 and last 47 nt of each read, filtering to keep only reads with 95% of nucleotides with a quality score of >28, alignment to the reference genome (BOWTIE, -q -p 8 -S -n 2 -e 70 -l 40 –maxbts 800 -y -k 1–best –phred33-quals) (24), sorting of the aligned reads and removal of PCR duplicates, random down sampling (40%) of the input to compensate for the smaller number of unique aligned reads in the ChIP sample (PICARD; http://picard.sourceforge.net), and peak finding (MACS and HOMER) (25, 26).

Assay of β-galactosidase activity in yeast. Exponentially growing cells (1 OD_{600} unit) were resuspended in 350 μl of culture medium, flash-frozen in liquid nitrogen, and thawed at room temperature. β-Galactosidase activity was assayed using the yeast β-galactosidase assay kit (Pierce, Rockford, IL), as described in the manufacturer's manual, at 37°C for 1 h.

RESULTS

Nts1 is a nuclear protein with roles in maintaining genome stability. To shed light on how the structural maintenance of chromosome complex Smc5-Smc6 functions, we carried out a genetic screen for high-copy-number suppressors of a mutation in its Nse5 subunit, which will be described in detail elsewhere. This screen produced several hits, one of which was the hypothetical gene *SPCC24B10.19C*, here called *nts1* (*nse5*^{ts} suppressor 1). *nts1* codes for a protein that localized to the nucleus, with some cells displaying a "focus" of Nts1 near the nucleolar rim (Fig. 1A). Deleting *nts1* by replacing its open reading frame with a selectable marker (27) produced viable cells. Although unchallenged *nts1*Δ cells grew as well as the wild type, they were sensitive to relatively high concentrations of the ribonucleotide reductase inhibitor hy-

droxyurea (HU) and the topoisomerase I poison camptothecin (CPT) but not UV light (Fig. 1B). We also found that they were somewhat resistant to the microtubule-depolymerizing agent thiabendazole (TBZ).

The most striking genome stability phenotype related to *nts1* is observed upon its overexpression, rather than deletion, which causes only mild genotoxin sensitivities. Overexpressing *nts1*$^+$ dramatically rescued the sensitivity to DNA-damaging agents of *nse5*Δ and *nse6*Δ mutants (Fig. 1C). Nse5 and Nse6 are two nonessential core subunits of the Smc5-Smc6 complex. They form an obligate dimer within the larger complex that deals with blocks to replication fork progression by as-yet-undefined mechanisms, which depend on homologous recombination (28). This phenotype is strikingly specific, because overexpressing *nts1*$^+$ did not rescue the genome instability of Smc5-Smc6 mutants other than *nse5*Δ or *nse6*Δ (Fig. 1C) or other DNA repair mutants (data not shown). Thus, *nts1*$^+$ overexpression specifically bypasses the unique functions of Nse5-Nse6 within the larger Smc5-Smc6 complex. Overall, these results show that Nts1 is a nuclear protein that plays a role in the cellular response to genotoxins.

Nts1 is part of the Clr6 HDAC. In order to gain insight into the potential roles of Nts1, we affinity purified it from whole-cell extracts of cells producing $FLAG_3$-Nts1-TAP and analyzed its associated proteins by multidimensional protein identification technology (MudPIT). Extracts from wild-type cells served as a control to identify the proteins that spuriously carried through the purification. We identified 268 proteins in the $FLAG_3$-Nts1-TAP purification. Twenty-four of these were observed in the control sample and were disregarded *a priori*. Highly abundant proteins that commonly copurify with affinity-purified protein, e.g., ribosomal proteins, were also screened out. Many of the remaining top hits, noted by footnote *c* in Table 2, were known components of the Clr6 HDAC, such as Sds3, Prw1, PstI/3, Rtx2/3, and Laf1/2 (5, 29). In addition, the forkhead transcription factor Fkh2, which is known to interact with the budding yeast Rpd3 HDAC (30), and the uncharacterized proteins Mug165 and Png3 were also highly represented. To verify that Nts1 is part of the Clr6 HDAC, we appended a TAP tag to the endogenous *nts1* gene in a strain where *clr6* had been fused to a myc_{13} epitope, and vice versa, and carried out TAP tag pulldowns followed by Western blotting. These assays confirmed that Nts1 did indeed interact with Clr6 (Fig. 2A) and vice versa (Fig. 2B). Our mass spectrometry analysis also identified multiple subunits of three other complexes: the regulatory cap of the proteasome (Rpt3 to Rpt6), the RSC (Rsc58 and Ssr3), and INO80 (Rvb1/2) chromatin-remodeling complexes. Yet, we did not detect any of these three complexes in Nts1-TAP immunoprecipitates by Western blotting (data not shown). This is consistent with the fact that such complexes are relatively poorly represented at the peptide level in the mass spectrometry data set (Table 2). Therefore, we conclude that Nts1 is a genuine and novel component of the Clr6 HDAC.

Nts1, Mug165, and Png3 define a new variant of Clr6 complex I. Since the Clr6 HDAC subunits that copurified with Nts1 (Table 1) specifically belonged to complex I (Sds3, Prw1, PstI/3, Rtx2/3, Laf1/2) but not complex I′ (Cti6, Dep1, and Png2) or complex II (Pst2, Alp13, Cph1/2) (5, 29), we hypothesized that Nts1 defined a unique Clr6 complex I entity. In fact, Western blotting of immunoprecipitated Png2 or Alp13, as representative members of complex I′ and II, respectively, showed very little, if any, recovery of Nts1 (Fig. 3A). On the other hand, Clr6, which served as a positive control, strongly coprecipitated with both Png2 and Alp13. Thus, the Nts1-Clr6 complex is distinct from complexes I′ and II.

In addition to pulling down several components of the Clr6 HDAC, Nts1 strongly copurified with Mug165 and Png3

TABLE 2 List of proteins that were detected by mass spectrometry in a pulldown of Nts1[a]

Protein	Gene ID	NSAFe5 score[d]		Rank no.
		$FLAG_3$-Nts1-TAP PD	Control PD	
Nts1[b]	SPCC24B10.19c	5211	0	8
Sds3[c]	SPAC25B8.02	2942	0	13
Prw1[c]	SPAC29A4.18	2319	0	18
Clr6[c]	SPBC36.05c	1916	0	21
Mug165[c]	SPAC5D6.02c	1747	0	22
Png3[c]	SPAC16E8.12c	1628	0	24
PstI[c]	SPBC12C2.10c	1020	0	47
Pst3[c]	SPBC1734.16c	674	0	65
Fkh2[c]	SPBC16G5.15c	631	0	69
Rtx3[c]	SPCC1259.07	577	0	71
Histone H2B	SPCC622.09	399	0	94
Laf2[c]	SPCC1682.13	324	0	98
Rxt2[c]	SPBC428.06c	300	0	100
Histone H4	Multiple	163	0	120
Laf1[c]	SPAC14C4.12c	136	0	126
Rad25	SPAC17A2.13c	129	0	127
Rad24	SPAC8E11.02c	129	0	128
Nop56	SPBC646.10c	93	0	133
Mlo3	SPBC1D7.04	77	0	137
Histone H2A	Multiple	74	0	138
HMG box protein	SPBC28F2.11	63	0	142
Rvb1	SPAPB8E5.09	61	0	144
Rpt4	SPCC1682.16	58	0	146
Tcg1	SPBC660.11	32	0	156
Rpt3	SPCC576.10c	29	0	161
Meu27	SPCC1259.14c	28	0	162
Rpt6	SPBC23G7.12c	28	0	163
Predicted ubiquitin ligase subunit	SPBC106.13	28	0	164
Nop58	SPAC23G3.06	28	0	165
Rpt5	SPAC3A11.12c	26	0	169
Oga1	SPBC16A3.08c	25	0	172
Rsc58	SPAC1F3.07c	24	0	173
Predicted human LYAR homologue	SPBC215.06c	24	0	177
Cpc2	SPAC6B12.15	22	0	181
Ump1	SPCC14G10.03c	22	0	184
Ssr3	SPAC23G3.10c	16	0	199
Rvb2	SPBC83.08	15	0	205
But2	SPBC3D6.02	14	0	209
Rpn11	SPAC31G5.13	9	0	232
Tci1	SPBC16D10.01c	8	0	235
Tubulin (β subunit)	SPBC26H8.07c	6	0	241
Tubulin (α subunit)	Multiple	6	0	242
Rsc4	SPBC1734.15	5	0	249
Cdc22	SPAC1F7.05	3	0	258
Cdc48	SPAC1565.08	3	0	259

[a] Nts1 interacts with several components of the Clr6 HDAC.
[b] Target protein subjected to affinity purification.
[c] Top hits that are known components of the Clr6 HDAC.
[d] PD, pulldown. NSAFe5 is a semiquantitative assessment of protein abundance.

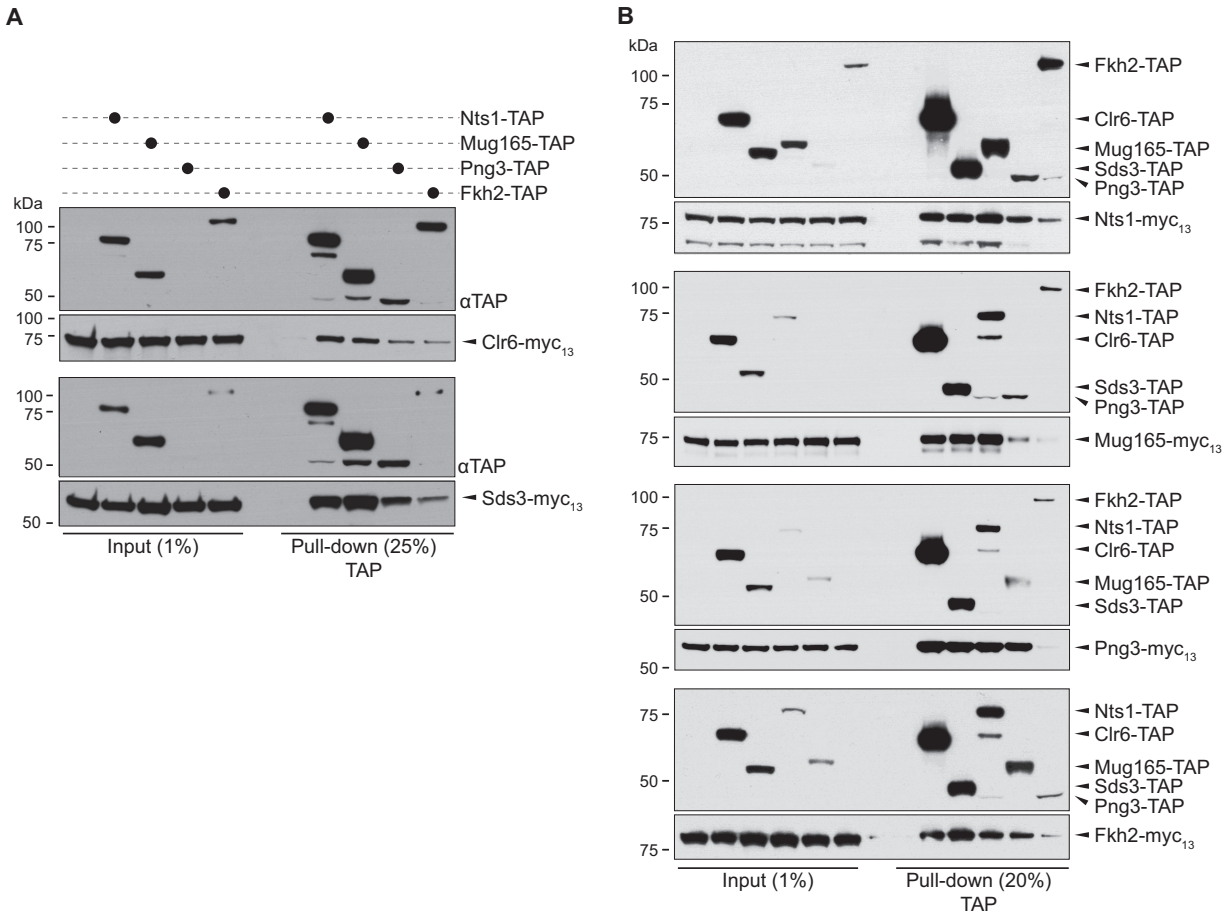

FIG 2 Nts1, Mug165, Png3, and Fkh2 are integral components of the Clr6 HDAC. (A and B) TAP-tagged proteins were captured on IgG-Sepharose from whole-cell lysates of strains producing the indicated TAP- and Myc-tagged proteins and analyzed by peroxidase-antiperoxidase and anti-Myc Western blotting. Input samples were 1% of the total protein used in the pulldown. For the pulldown samples, we loaded 20% (or 25%) (vol/vol) of the IgG resin eluate.

(Table 2), two previously uncharacterized proteins. We thus asked if they are also part of the Nts1-Clr6 complex by testing if they interact with Clr6, the complex I-specific subunits Sds3, Nts1, and each other. Figures 2A and B show that Mug165 and Png3 indeed physically interact with complex I, i.e., Sds3, Nts1, and each other. In light of these results, we examined if Nts1, Mug165, and Png3 associated, as an independent unit, with the core subunits of complex I. In order to address this question, we used immunoprecipitation followed by Western blotting to assess how individually deleting *nts1*, *mug165*, or *png3* affected the physical interaction between the remaining two subunits with either each other or Sds3, as a representative core subunit of complex I. We found that deleting either *png3* or *nts1* did not affect the interactions between Mug165 and either Nts1 or Png3 or that between Sds3 and Mug165 (Fig. 3B). On the other hand, deleting *mug165* abolished the interactions of both Nts1 and Png3 with Sds3, i.e., the core of complex I, and that between Png3 and Nts1 (Fig. 3C).

Overall, these results show that Nts1 and Png3, via Mug165, interact with the core components of complex I to define a unique Clr6 HDAC entity, which we named complex I′′. Genetic analyses corroborate the proposed molecular architecture of complex I′′, because deletion of *mug165* is epistatic to *nts1* with respect to DNA damage sensitivity (Fig. 3D).

Nts1 controls the RNA levels of subtelomeric, Tf2, and noncoding RNA genes via Clr6. Clr6 has established roles in controlling gene expression by modulating histone acetylation (4, 5). Therefore, we asked if Nts1 similarly regulates gene expression. Using high-definition 44K arrays that include almost all of the known or predicted fission yeast open reading frames and other genetic elements, we compared the global RNA transcript levels of wild-type cells to those of the *nts1*Δ *mug165*Δ *png3*Δ triple mutant and cells overexpressing $nts1^+$ ($nts1^+$ O/E). These data can be accessed at www.ebi.ac.uk/arrayexpress by using accession number E-MTAB-2543. We found that deleting *nts1*, *mug165*, and *png3* increased, by 1.5-fold or more, the RNA levels of 106 genes, including many whose expression is regulated under stress conditions, several membrane transporters, and some antisense transcripts (21, 22). We also observed that the *nts1*Δ *mug165*Δ *png3*Δ mutant had elevated levels of transcripts from repetitive sequences that are normally repressed in wild-type cells, such as *Tf2* retrotransposons and *wtf* elements, which are genes or pseudogenes that contain transmembrane domains and are flanked by *Tf2*-type long terminal repeats (LTRs) (31). As anticipated from our mass spectrometry data, comparison of the *nts1*Δ *mug165*Δ *png3*Δ expression signature with that of the temperature-sensitive Clr6 allele, *clr6-1* (9), revealed significant overlap in deregulated genes

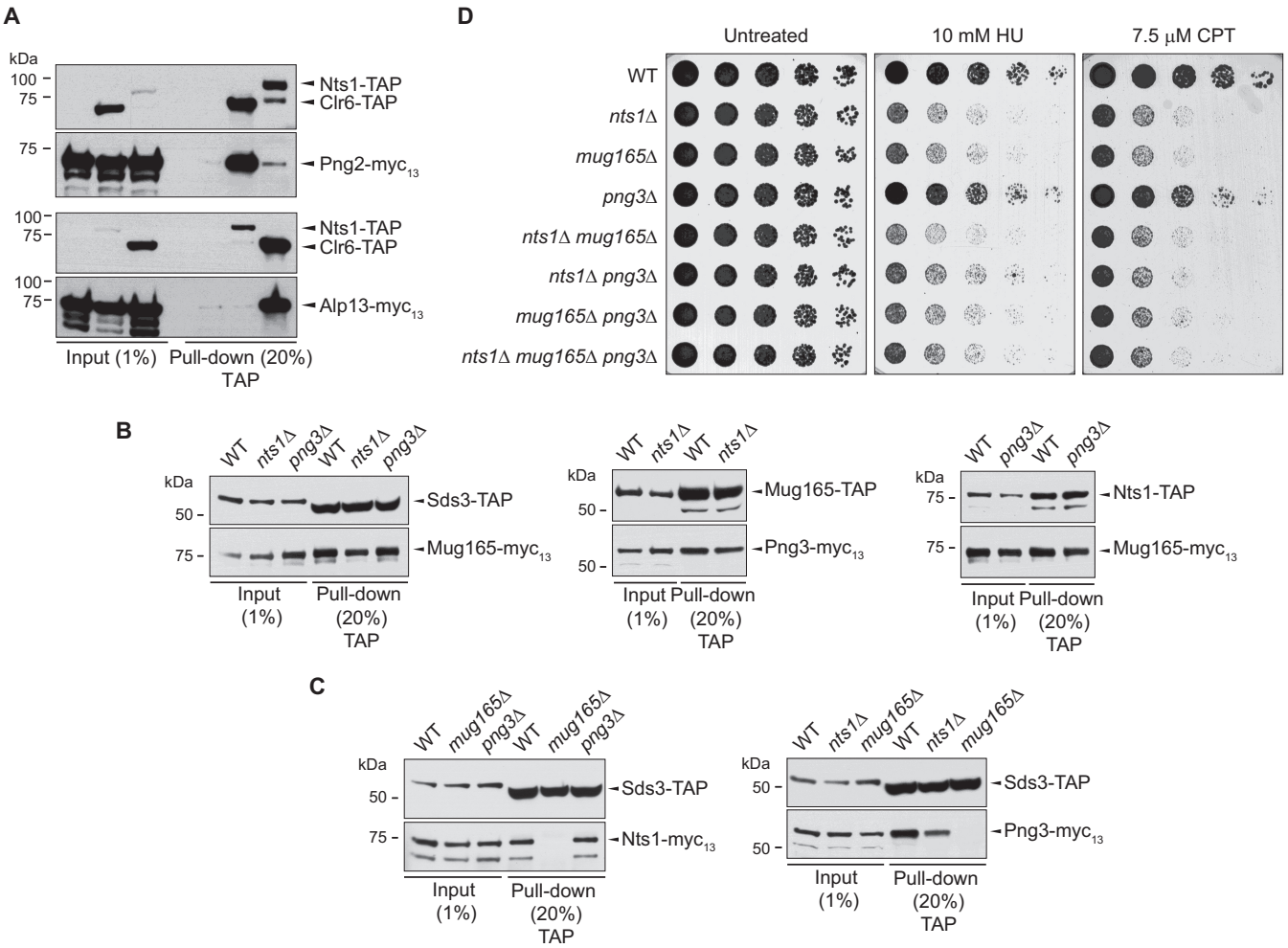

FIG 3 Architecture of the Clr6 HDAC containing Nts1, Mug165, and Png3. (A) Nts1 associates specifically with Clr6 complex I. TAP tag pulldowns were carried out on the strains producing the indicated epitope-tagged proteins as described for Fig. 2. (B and C) Mug165 mediates the interaction between Nts1 and Png3 and the core of Clr6 complex I. TAP tag pulldowns were carried out on the strains carrying the indicated epitope-tagged proteins and knockout alleles as described for Fig. 2. (D) *nts1* and *mug165* are epistatic with each other. The noted strains were serially diluted onto rich medium in the presence of the indicated drugs and grown at 30°C.

($P = 3 \times 10^{-12}$). Consistent with Nts1 constituting a variant of the Clr6 large complex, many more genes are deregulated in *clr6-1* than in *nts1*Δ *mug165*Δ *png3*Δ mutant cells. Significant overlap with Nts1-, Mug165-, and Png3-regulated genes was also observed in cells lacking the histone variant H2A.Z (*pht1*Δ; $P = 1.4 \times 10^{-15}$) (32) and the acetyltransferase Gcn5 (*gcn5*Δ; $P = 3.4 \times 10^{-15}$) (33). Notably, the levels of an unusually large number of long noncoding RNA genes, about 1/5 of the total number of upregulated genes, were increased in cells lacking Nts1, Mug165, and Png3.

In contrast, overexpressing *nts1* led to a reduction in transcripts from several loci, including those from the *Tf2* elements. Furthermore, many of the genes whose RNA levels were lowered by overexpressing *nts1* were upregulated in *nts1*Δ *mug165*Δ *png3*Δ cells (Table 3). When mapping all Nts1-, Mug165-, and Png3-regulated genes onto the three chromosomes of the fission yeast genome, we observed that they clustered at subtelomeric regions and/or were associated with solo *Tf2* LTRs. In fact, statistical analysis revealed a highly significant clustering of genes whose mRNA levels were upregulated by deleting *nts1* at the "right" telomere of chromosome I ($P < 0.05$) and at both telomeres of chromosome II ($P < 0.001$ for both telomeres). We did not detect any significant clustering at the subtelomeric regions of chromosome III, which is consistent with the fact that the rRNA genes occupy these loci. *Tf2* LTRs and solo LTRs also significantly overlapped with *nts1*-controlled genes (Table 4).

To validate our genome-wide analyses, we examined two hits from the Nts1-regulated gene pool in more detail, the *aes1* subtelomeric gene and the *Tf2* retrotransposons. By using reverse transcription coupled to quantitative PCR (RT-qPCR), we confirmed that *aes1* RNA levels were upregulated in *nts1*Δ *mug165*Δ *png3*Δ cells (Fig. 4B). An analogous effect was observed in the single *nts1*Δ and *mug165*Δ mutants, indicating that Nts1 function depends on it being tethered to the rest of the Clr6 HDAC core complex. Similarly, we found that in comparison to the wild type, the *Tf2* retrotransposase RNA levels were also increased in the *nts1*Δ, *mug165*Δ, and *nts1*Δ *mug165*Δ *png3*Δ mutants (Fig. 4B). Because *Tf2* elements are almost identical to each other, nucleic

TABLE 3 List of the genes that were upregulated in *nts1*Δ cells and downregulated in cells overexpressing *nts1*[a]

Gene name	Feature(s)
aes1	Subtelomeric
eno102	Subtelomeric and next to LTR
meu19 (*SPNCRNA.29*)	Subtelomeric and next to LTR
prl14 (*SPNCRNA.14*)	Next to LTR
SPAC57A7.05	Subtelomeric and next to LTR
SPAC750.01	Subtelomeric and next to LTR
SPAC977.14c	Subtelomeric
SPBC8E4.03	Subtelomeric and next to LTR
SPBPB2B2.01	Subtelomeric
SPBPB2B2.09c	Subtelomeric and next to LTR
SPCC569.07	Subtelomeric and next to LTR
SPCP20C8.03	Subtelomeric and next to LTR
SPNCRNA.1056	Next to LTR
SPNCRNA.1117	Next to LTR
SPNCRNA.1258	Next to LTR
SPNCRNA.1288	Subtelomeric and next to *Tf2-13*
SPNCRNA.1506	Next to LTR
SPNCRNA.1590	Next to LTR
SPNCRNA.252	
SPNCRNA.310	Subtelomeric
SPNCRNA.444	Subtelomeric and next to LTR
SPNCRNA.446	Subtelomeric
SPNCRNA.730	Next to LTR
SPNCRNA.860	Next to *Tf2-3*
SPNCRNA.976	Next to LTR
Tf2-1	
Tf2-10	
Tf2-11	Subtelomeric
Tf2-13	Subtelomeric
Tf2-3	
Tf2-8	
vht1	Near telomere

[a] By 1.5-fold or more in at least one of two independent hybridizations. Genes that are upregulated in cells lacking *nts1* and downregulated in those overexpressing it are found close to telomeres and/or *Tf2* elements.

acid hybridization or RT-qPCR techniques cannot distinguish between them. Thus, it was formally possible that the *nts1*Δ-dependent increase in *Tf2* RNA originated from deregulation of a single *Tf2* element, instead of derepressing all 13 of them. To test this possibility, we assessed how deleting *nts1* affected the repression state of *Tf2-2*, *Tf2-3*, *Tf2-10*, or *Tf2-11*, as representative members of the *Tf2* family of retrotransposons, by measuring β-galactosidase activity in wild-type and *nts1*Δ strains that contained an *lacZ* reporter under the control of each specific transposable element (11). Deleting *nts1* led to a statistically significant increase in *lacZ* reporter activity for *Tf2-2*, *Tf2-3*, and *Tf2-11*, albeit to various degrees, probably because of the different degrees of basal repression at each element. This suggests that complex I′′ does in fact impinge on all *Tf2* elements (Fig. 4C).

Using the transcriptional output of the *aes1* locus, we were also able to determine if Nts1's functions were mediated via Clr6. If so, then *clr6-1* and the *nts1*Δ mutation should be epistatic with respect to their transcriptional effects at *aes1*. Inactivating Clr6 using the *clr6-1* allele upregulated *aes1* RNA levels almost as much as deleting *nts1* alone. The magnitude of this effect was the same in the double *clr6-1 nts1*Δ and single *nts1*Δ mutants, which means that *nts1* and *clr6* are epistatic with each other (Fig. 4D). Thus, these results together with the physical interaction data indicate that *nts1* exerts its functions at the *aes1* locus via *clr6*, and vice versa.

Genome-wide localization of Nts1. Having determined that Nts1 controls the RNA levels of several genes, we asked if this function correlates with Nts1's physical localization across the genome. The genome-wide localization of Clr6 has not been determined, and that of its budding yeast homologue, Rpd3, is somewhat controversial (34, 35). In particular, Kurdistani et al. (34) found Rpd3 loading at highly transcribed genes, whereas Robert et al. (35) found that Rpd3 loading sites did not correlate with transcriptional rate but were enriched for cell cycle regulatory genes.

We performed ChIP for Nts1 followed by deep sequencing (ChIP-seq) to identify the DNA sequences with which Nts1 preferentially associates. Raw and processed ChIP-seq data can be accessed at www.ncbi.nlm.nih.gov/geo by using accession number GSE57040. Interestingly, a cursory visual inspection revealed no clear correlation between Nts1 binding sites along the genome and the genes that are deregulated upon *nts1* deletion (Fig. 4A and Table 3). However, statistical analyses revealed that Nts1 loading sites were enriched for cell cycle-regulated genes, as for Rpd3 in budding yeast (35), highly expressed genes, midmeiosis-induced genes, and Fkh2-bound genes, consistent with Nts1's presence in the same Clr6 complex I′′ (Table 5) (36–39). Potential loading sites were also apparent at tRNA and rRNA loci; however, directed ChIP-qPCR analyses did not support these assignments, which were likely spurious due to their repetitive nature and consequent assignment to multiple loci. Loading of Nts1 at the predominant *SPNCRNA.276* locus on chromosome I, as well as several other sites that were identified in our ChIP-seq analysis as "true" peaks, was confirmed by ChIP-qPCR (Fig. 4F). Localization to these loci is specific for Nts1 because the chromatin-associated Smc5-Smc6

TABLE 4 Statistical correlation between *nts1*-regulated genes and genes that directly overlap with *Tf2* LTRs and solo LTRs or are found within 500 bp of these elements[a]

Up- or downregulation	No. of genes associated with LTRs		*P* value		Median no. of genes randomly associated with LTRs (1,000 permutations)	
	Direct	500 bp	Direct	500 bp	Direct	500 bp
nts1$^+$ O/E ↓	14	17	2.23×10^{-11}	4.40×10^{-5}	1	1
*nts1*Δ ↑	16	34	3.49×10^{-12}	8.82×10^{-15}	1	1
*nts1*Δ ↑ *nts1*$^+$ O/E ↓	16	18	6.82×10^{-21}	1.04×10^{-12}	0	0

[a] Direct, genes that directly overlap with *Tf2* LTRs and solo LTRs; 500 bp, genes found within 500 bp of Tf2 LTRs. The median number of nucleus-encoded genes that randomly intersect with *Tf2* LTRs or are found within 500 bp of these loci is also shown.

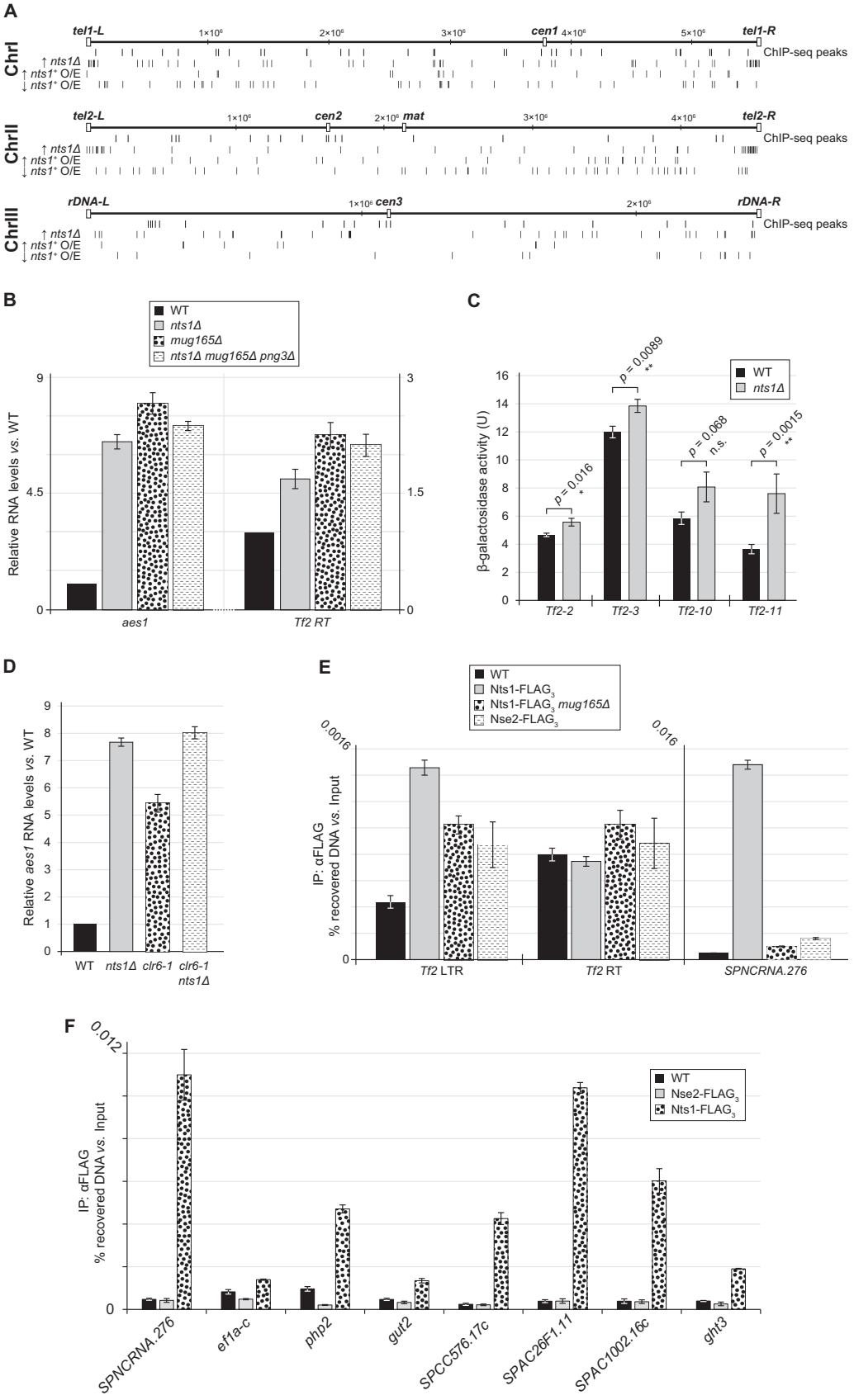
A
ChrI
tel1-L
cen1
tel1-R
ChIP-seq peaks
↑ nts1Δ
↑ nts1+ O/E
↓ nts1+ O/E
ChrII
tel2-L
cen2
mat
tel2-R
ChrIII
rDNA-L
cen3
rDNA-R
B
WT
nts1Δ
mug165Δ
nts1Δ mug165Δ png3Δ
Relative RNA levels vs. WT
aes1
Tf2 RT
C
β-galactosidase activity (U)
p = 0.0089
p = 0.016
p = 0.068
p = 0.0015
n.s.
Tf2-2
Tf2-3
Tf2-10
Tf2-11
D
Relative aes1 RNA levels vs. WT
WT
nts1Δ
clr6-1
clr6-1 nts1Δ
E
Nts1-FLAG3
Nts1-FLAG3 mug165Δ
Nse2-FLAG3
IP: αFLAG
% recovered DNA vs. Input
0.0016
0.016
Tf2 LTR
Tf2 RT
SPNCRNA.276
F
0.012
Nse2-FLAG3
Nts1-FLAG3
SPNCRNA.276
ef1a-c
php2
gut2
SPCC576.17c
SPAC26F1.11
SPAC1002.16c
ght3

TABLE 5 Statistical correlation between the genes found within 500 bp of Nts1 binding sites and other gene or target types

Gene or target type	Reference for data set	Overlap with referenced data set	*P* value
Top 10% most highly expressed genes	37	25 of 483 genes	4.2×10^{-15}
Genes flanking mitotic replication origins	54	19 of 481 genes	1.2×10^{-8}
Genes upregulated 2-fold or more upon oxidative stress	36	27 of 483 genes	8.1×10^{-14}
Targets of Fkh2 (as determined by ChIP-chip[a])	38	15 of 79 genes	2.0×10^{-16}
Top 300 cell cycle-regulated genes	38	30 of 300 genes	2.2×10^{-9}
Targets of Mei4	39	20 of 558 genes	1.8×10^{-8}

[a] ChIP-chip, chromatin immunoprecipitation with microarray technology.

complex subunit Nse2 (40) did not significantly copurify with DNA from such sites.

Despite the fact that Nts1 deletion or overexpression clearly "toggles" *Tf2* RNA levels, automated analysis of the ChIP-seq data did not assign Nts1 binding sites at these loci. However, DNA from the repetitive *Tf2* elements, and in particular their LTRs, was more heavily enriched in the Nts1 "ChIP" sample than in the "Input" material, which is a commonly used control for sequencing bias in ChIP-seq experiments. In light of this, we hypothesized that Nts1 may indeed bind at retrotransposable elements. We tested this using ChIP-qPCR, which revealed that Nts1 does indeed copurify with DNA from the LTRs of *Tf2* elements but not the intervening retrotransposase ORF (Fig. 4E). Thus, Nts1 localizes to several unique loci along the genome, including the *Tf2* LTRs.

Nts1 localizes to *SPNCRNA.276* independently of genomic context. We next used *SPNCRNA.276*, a hot spot of Nts1 chromatin association, as a "reporter" to determine if either broad genomic or local contexts direct Nts1 chromatin binding. To this end, we deleted the endogenous subtelomeric locus encompassing the ncRNA genes 276 and 30 (*SPNCRNA.276/0.30*) and inserted a copy of it (pNZ86) (Fig. 5A) at the unrelated euchromatic *leu1* locus. In addition, we integrated a longer fragment that included *SPNCRNA.1087* and the neighboring gene *SPAC1039.11c* (*gto1*; pNZ84) and a shorter one that contained only *SPNCRNA.276* at *leu1* (pNZ87) (Fig. 5A). Using these engineered loci, we found by ChIP-qPCR that Nts1 localized to the ectopic *SPNCRNA.276* sequence as well as it did to the endogenous locus for the longer construct (pNZ84) and somewhat less efficiently for the shorter one (Fig. 5B). Localization of Nts1 to *Tf2* LTRs, which we expected to be unaffected by moving the *SPNCRNA.276* locus, served as a control to confirm that ChIP efficiency was comparable among all four samples. These data show that genome binding by complex I′′ is not governed solely by genomic context, e.g., subtelomeric position, and may instead depend on a sequence-specific DNA binder in the complex.

Nts1 is unlikely to be the predicted sequence-specific DNA binder because deleting *mug165* abolished the interaction of Nts1 with *SPNCRNA.276*, while leaving its background binding to the *Tf2* retrotransposase ORF unchanged (negative control; Fig. 4E). In fact, this result, together with data demonstrating that Mug165 mediates the interactions of Nts1 and Png3 with the rest of the Clr6 core complex (Fig. 3C), indicates that Nts1 does not bind DNA directly. However, Nts1 probably plays an ancillary role in recruiting complex I′′ to the genome. We used ChIP-qPCR against Sds3, as a representative integral component of complex I′′, to examine how well it bound to the *SPNCRNA.276* gene, *Tf2* LTRs, and the *Tf2* retrotransposase ORF, as a negative control, in the *nts1*Δ and *nts1*Δ *mug165*Δ *png3*Δ backgrounds compared to the wild type. We found that, like Nts1, Sds3 also bound both the *SPNCRNA.276* gene and *Tf2* LTRs but not the *Tf2* retrotransposase ORF and that deleting *nts1* alone or *nts1* together with *mug165* and *png3* reduced, although did not abolish, the binding of Sds3 to both the *SPNCRNA.276* gene and *Tf2* LTRs (Fig. 5C). Overall, these data indicate that Clr6 I′′ loading at *SPNCRNA.276*, and likely at other loci, depends on one or more sequence-specific DNA binders, as suggested for Rpd3 in budding yeast.

Nts1 controls the levels of H3K9ac at *aes1*. Compromising the function of complex I preferentially increases the levels of acetylated lysine 9 of histone H3 (H3K9ac), a histone modification associated with transcriptionally active chromatin, across gene promoters (5). Together with the finding that Nts1, Mug165, and Png3 constitute a new complex I entity whose abrogation leads to increased RNA levels for several genes, we hypothesized that Nts1 antagonizes H3K9ac at these loci. The *aes1* gene was an ideal locus to test this hypothesis because its RNA levels were significantly upregulated by eliminating *nts1*. Therefore, we used ChIP-qPCR against H3K9ac at the *aes1* locus to determine any regulation by complex I′′. We confirmed the validity of this approach by demonstrating that in cells lacking the *clr4* histone methyltransferase gene, the H3K9ac levels at the outer centromeric repeat region (*otr*) were increased in comparison to those of the wild type (Fig. 6) (41). Similarly, we found that in the *nts1*Δ mutant, and equally in the *nts1*Δ *mug165*Δ *png3*Δ mutant, H3K9ac at the *aes1* locus was increased at least 2-fold. Interestingly, we did not detect any changes in H3K9ac levels at the *SPNCRNA.276* locus in *nts1*Δ cells

FIG 4 Nts1 controls the RNA levels of subtelomeric, *Tf2*, and ncRNA genes via Clr6. (A) Genome-wide localization of Nts1 protein (ChIP-seq peaks) and activity (bottom three lines) for the three fission yeast chromosomes. The three bottom lines show the distribution of the genes that were either upregulated (↑) or downregulated (↓) 1.5-fold or more by either deleting *nts1*, *mug165*, and *png3* (*nts1*Δ) or overexpressing it (*nts1*$^+$ O/E). (B) The RNA levels of *aes1* and the *Tf2* retrotransposase (*Tf2* RT) are increased in the *nts1*Δ, *mug165*Δ, and *nts1*Δ *mug165*Δ *png3*Δ mutants. qPCR was performed on cDNA derived from the indicated strains. RNA levels are expressed as average fold changes ± standard deviations, relative to the wild type and normalized to actin, using the cycle threshold ($\Delta\Delta C_T$) method. (C) Deletion of Nts1 leads to an increase in LacZ activity in *Tf2-lacZ* reporter strains. Strains harboring *lacZ* under the control of *Tf2-2*, *Tf2-3*, *Tf2-10*, or *Tf2-11* were harvested at mid-logarithmic phase and assayed for β-galactosidase activity. Each bar represents the mean from four independent experiments. Error bars represent the standard deviations. **, very statistically significant ($P < 0.01$); *, statistically significant ($P < 0.05$); n.s., not significant ($P > 0.05$). (D) The RNA levels of *aes1* are similarly upregulated in *nts1*Δ, *clr6-1*, and *nts1*Δ *clr6-1* cells. RNA levels were measured as described for panel B. (E and F) Nts1 copurifies with DNA from *Tf2* LTRs, *SPNCRNA.276*, and various other loci. Anti-FLAG ChIP assays were carried out on the indicated strains and analyzed by qPCR with primer sets annealing to *Tf2* LTRs, *Tf2* RT, *SPNCRNA.276*, *ef1a-c*, *php2*, *gut2*, *SPCC576.17c*, *SPAC26F1.11*, *SPAC1002.16c*, and *ght3*. The data are expressed as the average percentages of DNA recovery ± standard deviations relative to the amount of DNA in the input samples.

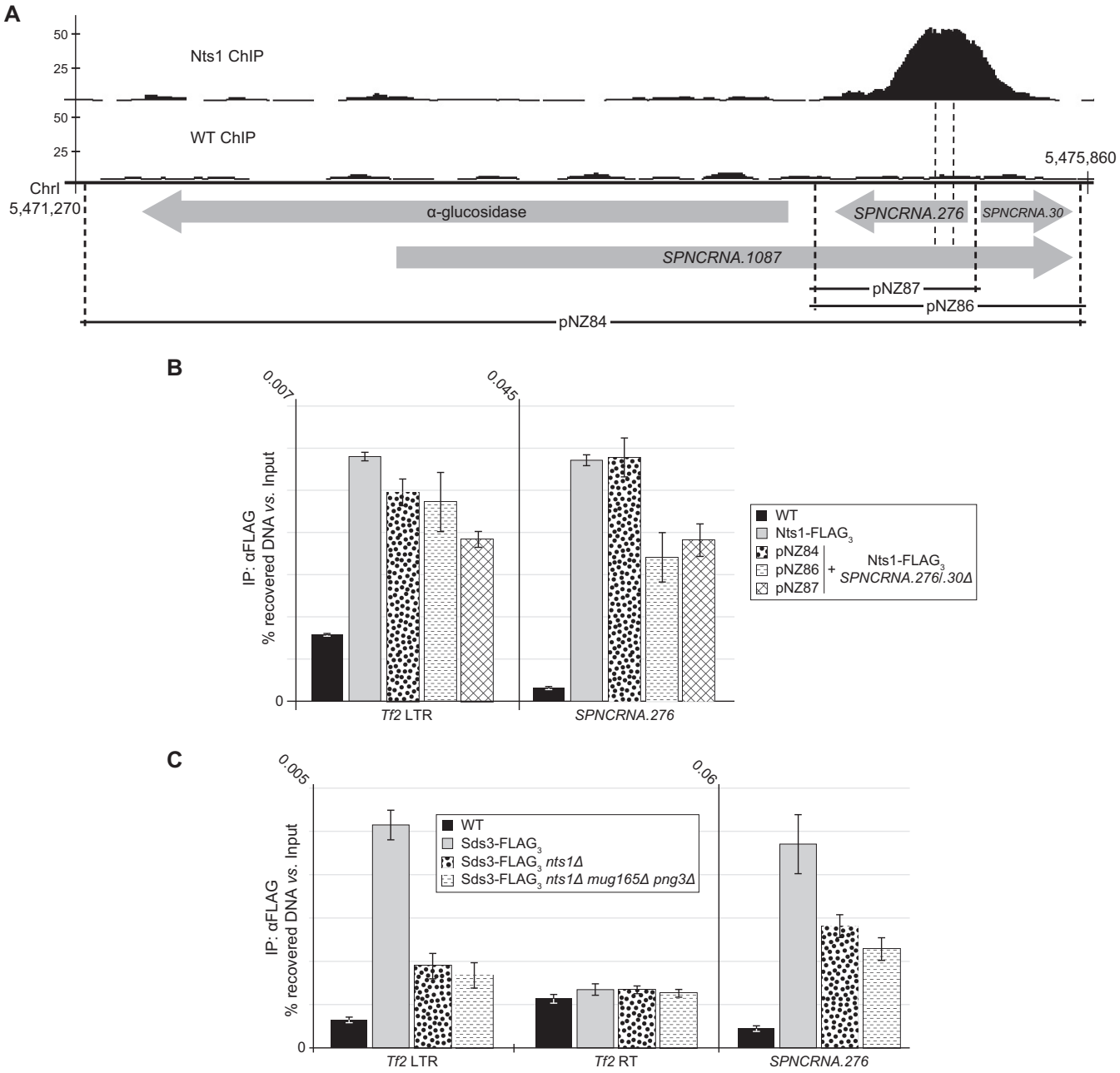

FIG 5 Nts1 localizes to *SPNCRNA.276* independently of its normal genomic context. (A) Schematic representation of the locus encompassing the α-glucosidase (*gto1*), *SPNCRNA.1087*, *SPNCRNA.276*, and *SPNCRNA.30* genes. The position at which Nts1 localizes within this region is shown as a ChIP-seq peak. The regions that were "transposed" to the *leu1* locus are shown and labeled as pNZ84, pNZ86, and pNZ87. Chromosome coordinates are expressed in bp. (B) Nts1 localizes to an ectopic *SPNCRNA.276* locus. Anti-FLAG ChIP assays were carried out as described in Fig. 4E. (C) Sds3 copurifies with DNA from *Tf2* LTRs and *SPNCRNA.276* in an *nts1*- and *mug165*-dependent manner. Anti-FLAG ChIP assays were carried out as described for Fig. 4E.

even though Clr6 is also present at this site, as determined by ChIP-qPCR (Fig. 6B).

DISCUSSION

Epigenetic regulation plays critical roles in controlling cell regulation. Here, we identify and functionally characterize Nts1, a novel epigenetic regulator important for genome stability in fission yeast. Through proteomic, biochemical, and genetic analyses, we determine that Nts1, together with Mug165 and Png3, defines a novel complex containing the evolutionarily conserved Clr6 histone deacetylase.

Consistent with functions previously ascribed to Clr6, cells lacking Nts1 exhibit increased transcriptional activity of genes that are normally repressed during rapid vegetative growth. Genes regulated by Nts1 are predominantly subtelomeric, or associated with the LTRs of *Tf2* retrotransposons. However, compared to Clr6 dysfunction (9), Nts1 deletion deregulates many fewer genes genome-wide and does not cause increased antisense transcrip-

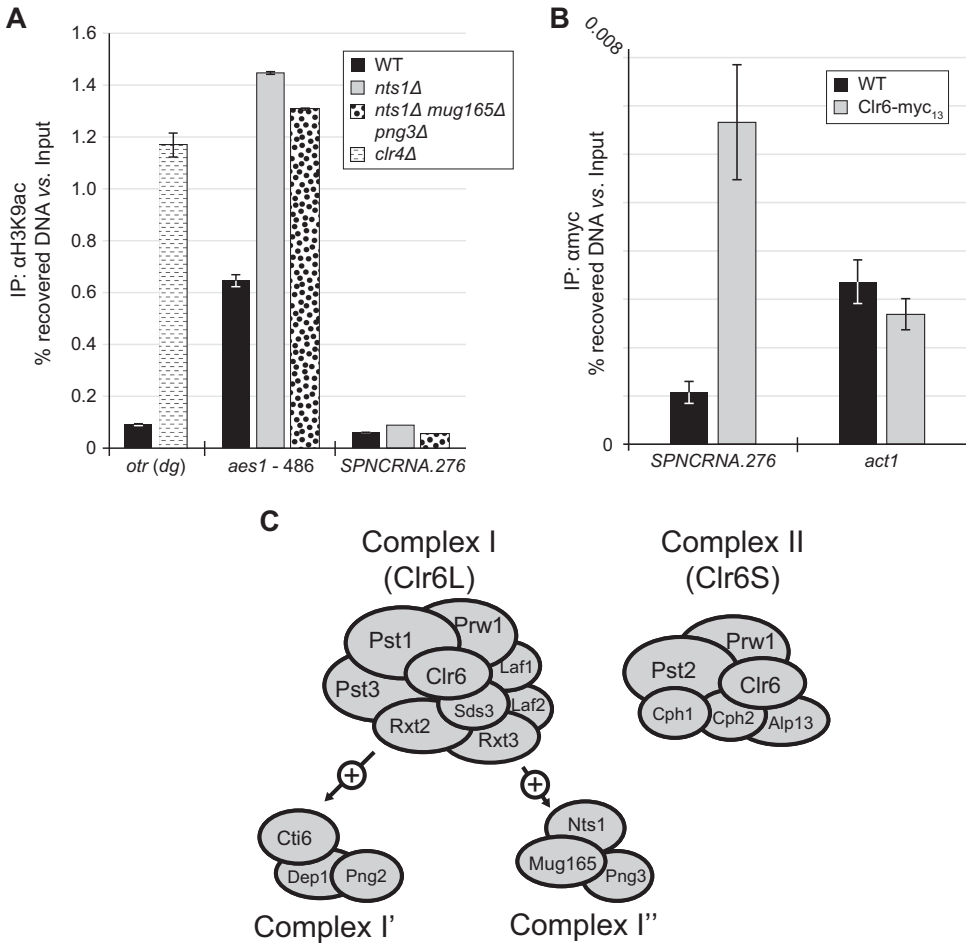

FIG 6 (A) Deletion of *nts1* leads to an increase in H3K9ac levels at the *aes1* promoter. Anti-H3K9ac ChIP assays were carried out on the indicated strains and analyzed by qPCR with primer sets annealing to the *dg* repeat found within the *otr*, a locus found approximately 486 bp upstream of *aes1*'s start codon (*aes1* promoter) and *SPNCRNA.276*. (B) Clr6 copurifies with DNA from *SPNCRNA.276*. ChIP assays were carried out on the indicated strains and analyzed by qPCR with primer sets annealing to *SPNCRNA.276* and *act1*. (C) Schematic representation of complexes I (core subunits, Clr6L, analogous to Rpd3L in budding yeast), I′, I′′, and II (Clr6S, analogous to Rpd3S in budding yeast).

tion at the centromere or other loci. Thus, Nts1 provides a new functional subdivision within the known Clr6 holocomplexes.

Cells lacking Nts1 are mildly sensitive to chronic replication stress induced by hydroxyurea and the topoisomerase inhibitor camptothecin but not UV light. These results echo those for Clr6 complexes I/I′ and II that are differentially sensitive to DNA-damaging agents (5), but within this group *nts1*Δ cells display a unique spectrum of sensitivities. Transcription profiling of *nts1*Δ cells did not reveal any significant changes in the expression of DNA damage response factors, suggesting that disruption of normal chromatin architecture likely underlies these *nts1*Δ cellular phenotypes, as concluded for other Clr6 complex mutants (5). Likewise, the reproducible relative resistance of *nts1*Δ cells to TBZ may reflect mitigating changes in chromatin and kinetochore structure or function; however, we cannot exclude the involvement of nonchromatin acetylated targets, such as tubulin. Unlike the relatively mild sensitivity to DNA damage exhibited by the *nts1*Δ mutant, overexpressing $nts1^+$ potently and specifically rescued the genome stability phenotypes of Nse5-Nse6 mutants. This dimer is an integral component of the larger Smc5-Smc6 complex. It plays roles in replication fork stability through as-yet-undefined mechanisms, which probably rely on homologous recombination. Future characterization of how $nts1^+$ overexpression bypasses the functions of Nse5-6 will likely shed light on the mechanisms of Smc5-Smc6. Clr6 associates with unique sets of proteins to define two functionally distinct complexes: complex I and II (5). The budding yeast Clr6 orthologue Rpd3 forms analogous ensembles, known as Rpd3L and Rpd3S, which share significant subunit composition with, and function similarly to, complexes I and II, respectively (29, 42–44) (Table 6). The ING family protein Png2 binds to the core of complex I and defines a variant known as complex I′ (5), whose functional distinction from the core complex remains unknown. We found that Nts1 coprecipitated with two previously uncharacterized proteins, Mug165 and Png3, as well as all of the subunits of complex I, except Png2, Dep1, and Cti6. We also showed that Mug165 bridges the binding of Png3 and Nts1 to the rest of the Clr6 HDAC. Thus, we propose that Nts1, Mug165, and Png3 define a variant of complex I that is distinct from complex I′, which we named complex I′′ (Fig. 6C).

Clr6 associates with unique sets of proteins to define two functionally distinct complexes: complex I and II (5). The budding yeast Clr6 orthologue Rpd3 forms analogous ensembles, known as

TABLE 6 Members of the known Clr6-containing complexes in fission yeast (*S. pombe*, complexes I and II) and their orthologues in budding yeast[a]

Complex	*S. pombe* orthologue(s)	*S. cerevisiae* orthologue(s)
II, Rpd3S	Clr6	Rpd3
	Pst2	Sin3
	Cph1, Cph2	Rco1
	Alp13	Eaf3
	Prw1	Ume1
I, Rpd3L		
Core	Clr6	Rpd3
	PstI, Pst3	Sin3
	Rxt2	Rxt2
	Rxt3	Rxt3
	Sds3	Sds3
	Prw1	Ume1
	Laf1, Laf2	YAL034C (?), YOR338W (?)
?	?	Sap30
	?	Ume6
	?	Dot6
	?	Tod6
	?	Ash1
I′	Cti6	Cti6
	Png2	Pho23
	Dep1	Dep1
I′′	Nts1	?
	Mug165	?
	Png3	?

[a] ?, unknown component.

Rpd3L and Rpd3S, which share significant subunit composition with, and function similarly to, complexes I and II, respectively (29, 42–44). The ING family protein Png2 binds to the core of complex I and defines a variant known as complex I′ (5), whose functional distinction from the core complex remains unknown. We found that Nts1 coprecipitated with two previously uncharacterized proteins, Mug165 and Png3, as well as all of the subunits of complex I, except Png2, Dep1, and Cti6. We also showed that Mug165 bridges the binding of Png3 and Nts1 to the rest of the Clr6 HDAC. Thus, we propose that Nts1, Mug165, and Png3 define a variant of complex I that is distinct from complex I′, which we named complex I′′.

The fact that *png2*Δ cells are not sensitive to DNA-damaging agents such as HU or camptothecin (5), whereas those lacking Nts1 are, suggests that complex I′ and complex I′′ likely have distinct molecular functions. Although Png3 is annotated as an ING family protein, it does not have the C-terminal plant homeodomain (PHD)-type zinc finger that distinguishes these proteins. Instead, Png3's N terminus is similar to human ING5 ($P = 6 \times 10^{-25}$, Ψ-BLAST BLOSUM62) and the budding yeast Rpd3L component and Png2 orthologue, Pho23 ($P = 1 \times 10^{-14}$, Ψ-BLAST BLOSUM62). Mug165, whose mRNA levels are upregulated during meiosis (metaphase I) (45) but which is also expressed during mitotic growth (Fig. 2), displays similarity to the complex I subunit Dep1 (*S. pombe* Dep1, $P = 4 \times 10^{-12}$, Ψ-BLAST BLOSUM62; *Saccharomyces cerevisiae* Dep1, $P = 1 \times 10^{-5}$, Ψ-BLAST BLOSUM62), which we did not detect in the pulldown of Nts1, thus raising the possibility that Mug165 and Dep1 execute analogous functions in complexes I′ and I′′, respectively. Phylogenetic analysis retrieved likely orthologues of Mug165 and Nts1 in *Schizosaccharomyces octosporus* (UniProt identifier [ID] S9RDA9 and S9Q448) and *Schizosaccharomyces cryophilus* (UniProt ID S9X7K7 and S9XB69), two fission yeast species closely related to *S. pombe*. Although the degree of identity among these proteins is obvious, they are surprisingly divergent given the evolutionary closeness of the three species. Therefore, in this context, structure and function likely count more than primary sequence, which could explain why clear orthologues of Mug165 and Nts1 are not found in budding yeast or humans.

Nts1 is a central player in complex I′′ because deleting it sensitizes cells to genotoxins to the same extent as decoupling it from the rest of the Clr6 HDAC, by deleting *mug165*. The mechanisms by which these HDACs are recruited to DNA remain unknown, but they could involve sequence-specific DNA-binding proteins, as in the case of the Abp1-mediated recruitment of Clr3 to the silent mating-type locus (8) and/or possibly epigenetic mechanisms (7). Nts1 might have been one such factor. However, this is unlikely, because when Nts1's interaction with the Clr6 core complex is disrupted, Nts1 cannot bind to *Tf2* LTRs or the *SPNCRNA.276* locus. Fkh2 could be a plausible alternative, because in budding yeast it recruits Rpd3L to the *CTS1* promoter (46), and there is significant overlap between the genome-wide loading profiles of Nts1 and Fkh2 (Table 5). Because only 15 out of the 79 loading sites of Fkh2 are also bound by Nts1, it would appear that additional DNA-binding proteins or recruitment mechanisms facilitate Clr6 complex I′′ loading. This would be consistent with studies of Rpd3 in budding yeast, which is recruited by different DNA binding factors to specific loci (35).

Intriguingly, Nts1 loading sites genome-wide do not correlate with the genes whose expression is deregulated upon Nts1 deletion. A similar lack of correlation between the genome-wide loading of Rpd3 in budding yeast and the loci that it regulates was also observed (34, 35). We validated our ChIP-seq analyses using ChIP-qPCR analysis of both Nts1 and the Clr6 complex I/I′/I′′ component Sds3 at various Nts1 "bound" loci. However, given that Nts1 apparently "loads" at some highly expressed genes that have been found to be "hyper-ChIPable" (47), we cannot exclude the possibility that some of the ChIP-seq peaks at such loci are not true sites at which Nts1 localizes.

Given the significant overlap in genes and loci regulated by Nts1 and Clr6, this raises interesting questions about Clr6 complex dynamics. To our knowledge, Clr6 binding sites have not been published, and histone deacetylation/acetylation has instead been used as a surrogate to indicate where in the genome it has been. Thus, it is possible that large-scale changes in chromatin packaging and architecture caused by Clr6 or Nts1 inactivation lead indirectly to the loss of transcriptionally repressive histone marks at certain loci (e.g., by increased access for acetyltransferases). The subtelomeric clustering and *Tf2* LTR proximity of the majority of Nts1, and many Clr6, coregulated loci could support such a model, given that these genomic features are organized in transcriptionally repressive subnuclear domains (e.g., see reference 12). In this regard, long-range interactions mediated by complex I′′ are a possibility (48, 49). Alternatively, complex I′′ may dynamically associate with the genes deregulated by deleting Nts1, and the threshold for significance in our ChIP-seq analyses may have obscured such associations. However, we did not detect loading of Nts1 at the *aes1* locus, whose expression and acetylation are both impacted by Nts1, whereas Nts1 and Clr6 load at the

SPNCRNA.276 locus but do not appear to affect either acetylation or expression of this locus. It is noteworthy that *SPNCRNA.276* is in the promoter region of the *gto1* gene that is induced in mid-meiosis by the meiosis-specific Mei4 transcription factor (50), and Mei4 target genes were enriched among the Nts1 binding sites (Table 5). Thus, it is possible that regulatory defects at the *gto1* locus in *nts1*Δ cells would be detected only during meiotic induction. Further experiments are required to unequivocally differentiate between direct and indirect transcriptional effects mediated by the Clr6 complex I′′.

We detected significant binding of Nts1 at the LTRs of *Tf2* retrotransposons by ChIP-qPCR; also, Nts1 deletion or overexpression results in transcriptional derepression or repression of *Tf2* elements, respectively. *Tf2* elements are transcriptionally derepressed in *clr6-1* mutants as well and in cells lacking the CENP-B-like protein Abp1 or the histone chaperone HIRA (8, 9, 11). That increased dosage of Nts1 represses *Tf2* elements is intriguing. It is possible that Nts1 drives the formation and/or stabilization of the transcriptionally repressive *Tf* bodies into which these potentially deleterious genetic elements are packaged (8, 12). Loss of such *Tf2*-repressive mechanisms in *nts1*Δ cells could contribute to their genotoxin sensitivity. As *Tf2* LTRs are dispersed throughout the genome and are highly similar, they can drive genomic instability through replication and recombination-based mechanisms (51), which would be exacerbated following genotoxic challenge.

ACKNOWLEDGMENTS

M.N.B. is supported by a Scholar Award from the Leukemia & Lymphoma Society. This study was funded by NIH grants GM068608 and GM081840 awarded to M.N.B., a Wellcome Trust Senior Investigator Award (grant number 095598/Z/11/Z) to J.B., and NIH grant GM089778 to J.A.W.

REFERENCES

1. **Dawson MA, Kouzarides T.** 2012. Cancer epigenetics: from mechanism to therapy. Cell **150:**12–27. http://dx.doi.org/10.1016/j.cell.2012.06.013.
2. **Haberland M, Montgomery RL, Olson EN.** 2009. The many roles of histone deacetylases in development and physiology: implications for disease and therapy. Nat. Rev. Genet. **10:**32–42. http://dx.doi.org/10.1038/nrg2485.
3. **Lee KK, Workman JL.** 2007. Histone acetyltransferase complexes: one size doesn't fit all. Nat. Rev. Mol. Cell Biol. **8:**284–295. http://dx.doi.org/10.1038/nrm2145.
4. **Grewal SI, Bonaduce MJ, Klar AJ.** 1998. Histone deacetylase homologs regulate epigenetic inheritance of transcriptional silencing and chromosome segregation in fission yeast. Genetics **150:**563–576.
5. **Nicolas E, Yamada T, Cam HP, Fitzgerald PC, Kobayashi R, Grewal SI.** 2007. Distinct roles of HDAC complexes in promoter silencing, antisense suppression and DNA damage protection. Nat. Struct. Mol. Biol. **14:**372–380. http://dx.doi.org/10.1038/nsmb1239.
6. **Sinha I, Wiren M, Ekwall K.** 2006. Genome-wide patterns of histone modifications in fission yeast. Chromosome Res. **14:**95–105. http://dx.doi.org/10.1007/s10577-005-1023-4.
7. **Grewal SI, Jia S.** 2007. Heterochromatin revisited. Nat. Rev. Genet. **8:**35–46. http://dx.doi.org/10.1038/nrg2008.
8. **Cam HP, Noma K, Ebina H, Levin HL, Grewal SI.** 2008. Host genome surveillance for retrotransposons by transposon-derived proteins. Nature **451:**431–436. http://dx.doi.org/10.1038/nature06499.
9. **Hansen KR, Burns G, Mata J, Volpe TA, Martienssen RA, Bahler J, Thon G.** 2005. Global effects on gene expression in fission yeast by silencing and RNA interference machineries. Mol. Cell. Biol. **25:**590–601. http://dx.doi.org/10.1128/MCB.25.2.590-601.2005.
10. **Anderson HE, Kagansky A, Wardle J, Rappsilber J, Allshire RC, Whitehall SK.** 2010. Silencing mediated by the *Schizosaccharomyces pombe* HIRA complex is dependent upon the Hpc2-like protein, Hip4. PLoS One **5:**e13488. http://dx.doi.org/10.1371/journal.pone.0013488.
11. **Anderson HE, Wardle J, Korkut SV, Murton HE, Lopez-Maury L, Bahler J, Whitehall SK.** 2009. The fission yeast HIRA histone chaperone is required for promoter silencing and the suppression of cryptic antisense transcripts. Mol. Cell. Biol. **29:**5158–5167. http://dx.doi.org/10.1128/MCB.00698-09.
12. **Lorenz DR, Mikheyeva IV, Johansen P, Meyer L, Berg A, Grewal SI, Cam HP.** 2012. CENP-B cooperates with Set1 in bidirectional transcriptional silencing and genome organization of retrotransposons. Mol. Cell. Biol. **32:**4215–4225. http://dx.doi.org/10.1128/MCB.00395-12.
13. **Moreno S, Klar A, Nurse P.** 1991. Molecular genetic analysis of fission yeast *Schizosaccharomyces pombe*. Methods Enzymol. **194:**795–823. http://dx.doi.org/10.1016/0076-6879(91)94059-L.
14. **Zilio N, Wehrkamp-Richter S, Boddy MN.** 2012. A new versatile system for rapid control of gene expression in the fission yeast *Schizosaccharomyces pombe*. Yeast **29:**425–434. http://dx.doi.org/10.1002/yea.2920.
15. **Wohlschlegel JA.** 2009. Identification of SUMO-conjugated proteins and their SUMO attachment sites using proteomic mass spectrometry. Methods Mol. Biol. **497:**33–49. http://dx.doi.org/10.1007/978-1-59745-566-4_3.
16. **Florens L, Washburn MP.** 2006. Proteomic analysis by multidimensional protein identification technology. Methods Mol. Biol. **328:**159–175. http://dx.doi.org/10.1385/1-59745-026-X:159.
17. **Eng JK, McCormack AL, Yates JR.** 1994. An approach to correlate tandem mass spectral data of peptides with amino acid sequences in a protein database. J. Am. Soc. Mass Spectrom. **5:**976–989. http://dx.doi.org/10.1016/1044-0305(94)80016-2.
18. **Tabb DL, McDonald WH, Yates JR, III.** 2002. DTASelect and contrast: tools for assembling and comparing protein identifications from shotgun proteomics. J. Proteome Res. **1:**21–26. http://dx.doi.org/10.1021/pr015504q.
19. **Cociorva D, D LT, Yates JR.** 2007. Validation of tandem mass spectrometry database search results using DTASelect. Curr. Protoc. Bioinform. Chapter **13:**Unit 13.14.
20. **Elias JE, Gygi SP.** 2007. Target-decoy search strategy for increased confidence in large-scale protein identifications by mass spectrometry. Nat. Methods **4:**207–214. http://dx.doi.org/10.1038/nmeth1019.
21. **Chen D, Toone WM, Mata J, Lyne R, Burns G, Kivinen K, Brazma A, Jones N, Bahler J.** 2003. Global transcriptional responses of fission yeast to environmental stress. Mol. Biol. Cell **14:**214–229. http://dx.doi.org/10.1091/mbc.E02-08-0499.
22. **Lyne R, Burns G, Mata J, Penkett CJ, Rustici G, Chen D, Langford C, Vetrie D, Bahler J.** 2003. Whole-genome microarrays of fission yeast: characteristics, accuracy, reproducibility, and processing of array data. BMC Genomics **4:**27. http://dx.doi.org/10.1186/1471-2164-4-27.
23. **Flicek P, Amode MR, Barrell D, Beal K, Billis K, Brent S, Carvalho-Silva D, Clapham P, Coates G, Fitzgerald S, Gil L, Giron CG, Gordon L, Hourlier T, Hunt S, Johnson N, Juettemann T, Kahari AK, Keenan S, Kulesha E, Martin FJ, Maurel T, McLaren WM, Murphy DN, Nag R, Overduin B, Pignatelli M, Pritchard B, Pritchard E, Riat HS, Ruffier M, Sheppard D, Taylor K, Thormann A, Trevanion SJ, Vullo A, Wilder SP, Wilson M, Zadissa A, Aken BL, Birney E, Cunningham F, Harrow J, Herrero J, Hubbard TJ, Kinsella R, Muffato M, Parker A, Spudich G, Yates A, Zerbino DR, Searle SM.** 2014. Ensembl 2014. Nucleic Acids Res. **42:**D749–D755. http://dx.doi.org/10.1093/nar/gkt1196.
24. **Langmead B, Trapnell C, Pop M, Salzberg SL.** 2009. Ultrafast and memory-efficient alignment of short DNA sequences to the human genome. Genome Biol. **10:**R25. http://dx.doi.org/10.1186/gb-2009-10-3-r25.
25. **Heinz S, Benner C, Spann N, Bertolino E, Lin YC, Laslo P, Cheng JX, Murre C, Singh H, Glass CK.** 2010. Simple combinations of lineage-determining transcription factors prime *cis*-regulatory elements required for macrophage and B cell identities. Mol. Cell **38:**576–589. http://dx.doi.org/10.1016/j.molcel.2010.05.004.
26. **Zhang Y, Liu T, Meyer CA, Eeckhoute J, Johnson DS, Bernstein BE, Nusbaum C, Myers RM, Brown M, Li W, Liu XS.** 2008. Model-based analysis of ChIP-Seq (MACS). Genome Biol. **9:**R137. http://dx.doi.org/10.1186/gb-2008-9-9-r137.
27. **Bahler J, Wu JQ, Longtine MS, Shah NG, McKenzie A, III, Steever AB, Wach A, Philippsen P, Pringle JR.** 1998. Heterologous modules for efficient and versatile PCR-based gene targeting in *Schizosaccharomyces pombe*. Yeast **14:**943–951.
28. **Pebernard S, Wohlschlegel J, McDonald WH, Yates JR, III, Boddy MN.** 2006. The Nse5-Nse6 dimer mediates DNA repair roles of the Smc5-Smc6 complex. Mol. Cell. Biol. **26:**1617–1630. http://dx.doi.org/10.1128/MCB.26.5.1617-1630.2006.
29. **Shevchenko A, Roguev A, Schaft D, Buchanan L, Habermann B, Sakalar**

C, Thomas H, Krogan NJ, Shevchenko A, Stewart AF. 2008. Chromatin central: towards the comparative proteome by accurate mapping of the yeast proteomic environment. Genome Biol. 9:R167. http://dx.doi.org/10.1186/gb-2008-9-11-r167.

30. Ho Y, Gruhler A, Heilbut A, Bader GD, Moore L, Adams SL, Millar A, Taylor P, Bennett K, Boutilier K, Yang L, Wolting C, Donaldson I, Schandorff S, Shewnarane J, Vo M, Taggart J, Goudreault M, Muskat B, Alfarano C, Dewar D, Lin Z, Michalickova K, Willems AR, Sassi H, Nielsen PA, Rasmussen KJ, Andersen JR, Johansen LE, Hansen LH, Jespersen H, Podtelejnikov A, Nielsen E, Crawford J, Poulsen V, Sorensen BD, Matthiesen J, Hendrickson RC, Gleeson F, Pawson T, Moran MF, Durocher D, Mann M, Hogue CW, Figeys D, Tyers M. 2002. Systematic identification of protein complexes in *Saccharomyces cerevisiae* by mass spectrometry. Nature 415:180–183. http://dx.doi.org/10.1038/415180a.
31. Bowen NJ, Jordan IK, Epstein JA, Wood V, Levin HL. 2003. Retrotransposons and their recognition of Pol II promoters: a comprehensive survey of the transposable elements from the complete genome sequence of *Schizosaccharomyces pombe*. Genome Res. 13:1984–1997. http://dx.doi.org/10.1101/gr.1191603.
32. Kim HS, Vanoosthuyse V, Fillingham J, Roguev A, Watt S, Kislinger T, Treyer A, Carpenter LR, Bennett CS, Emili A, Greenblatt JF, Hardwick KG, Krogan NJ, Bahler J, Keogh MC. 2009. An acetylated form of histone H2A.Z regulates chromosome architecture in *Schizosaccharomyces pombe*. Nat. Struct. Mol. Biol. 16:1286–1293. http://dx.doi.org/10.1038/nsmb.1688.
33. Helmlinger D, Marguerat S, Villen J, Gygi SP, Bahler J, Winston F. 2008. The *S. pombe* SAGA complex controls the switch from proliferation to sexual differentiation through the opposing roles of its subunits Gcn5 and Spt8. Genes Dev. 22:3184–3195. http://dx.doi.org/10.1101/gad.1719908.
34. Kurdistani SK, Robyr D, Tavazoie S, Grunstein M. 2002. Genome-wide binding map of the histone deacetylase Rpd3 in yeast. Nat. Genet. 31:248–254. http://dx.doi.org/10.1038/ng907.
35. Robert F, Pokholok DK, Hannett NM, Rinaldi NJ, Chandy M, Rolfe A, Workman JL, Gifford DK, Young RA. 2004. Global position and recruitment of HATs and HDACs in the yeast genome. Mol. Cell 16:199–209. http://dx.doi.org/10.1016/j.molcel.2004.09.021.
36. Chen D, Wilkinson CR, Watt S, Penkett CJ, Toone WM, Jones N, Bahler J. 2008. Multiple pathways differentially regulate global oxidative stress responses in fission yeast. Mol. Biol. Cell 19:308–317. http://dx.doi.org/10.1091/mbc.E07-08-0735.
37. Lackner DH, Beilharz TH, Marguerat S, Mata J, Watt S, Schubert F, Preiss T, Bahler J. 2007. A network of multiple regulatory layers shapes gene expression in fission yeast. Mol. Cell 26:145–155. http://dx.doi.org/10.1016/j.molcel.2007.03.002.
38. Marguerat S, Jensen TS, de Lichtenberg U, Wilhelm BT, Jensen LJ, Bahler J. 2006. The more the merrier: comparative analysis of microarray studies on cell cycle-regulated genes in fission yeast. Yeast 23:261–277. http://dx.doi.org/10.1002/yea.1351.
39. Mata J, Wilbrey A, Bahler J. 2007. Transcriptional regulatory network for sexual differentiation in fission yeast. Genome Biol. 8:R217. http://dx.doi.org/10.1186/gb-2007-8-10-r217.
40. McDonald WH, Pavlova Y, Yates JR, III, Boddy MN. 2003. Novel essential DNA repair proteins Nse1 and Nse2 are subunits of the fission yeast Smc5-Smc6 complex. J. Biol. Chem. 278:45460–45467. http://dx.doi.org/10.1074/jbc.M308828200.
41. Alper BJ, Job G, Yadav RK, Shanker S, Lowe BR, Partridge JF. 2013. Sir2 is required for Clr4 to initiate centromeric heterochromatin assembly in fission yeast. EMBO J. 32:2321–2335. http://dx.doi.org/10.1038/emboj.2013.143.
42. Keogh MC, Kurdistani SK, Morris SA, Ahn SH, Podolny V, Collins SR, Schuldiner M, Chin K, Punna T, Thompson NJ, Boone C, Emili A, Weissman JS, Hughes TR, Strahl BD, Grunstein M, Greenblatt JF, Buratowski S, Krogan NJ. 2005. Cotranscriptional Set2 methylation of histone H3 lysine 36 recruits a repressive Rpd3 complex. Cell 123:593–605. http://dx.doi.org/10.1016/j.cell.2005.10.025.
43. Carrozza MJ, Florens L, Swanson SK, Shia WJ, Anderson S, Yates J, Washburn MP, Workman JL. 2005. Stable incorporation of sequence specific repressors Ash1 and Ume6 into the Rpd3L complex. Biochim. Biophys. Acta 1731:77–87, discussion 75–76. http://dx.doi.org/10.1016/j.bbaexp.2005.09.005.
44. Carrozza MJ, Li B, Florens L, Suganuma T, Swanson SK, Lee KK, Shia WJ, Anderson S, Yates J, Washburn MP, Workman JL. 2005. Histone H3 methylation by Set2 directs deacetylation of coding regions by Rpd3S to suppress spurious intragenic transcription. Cell 123:581–592. http://dx.doi.org/10.1016/j.cell.2005.10.023.
45. Mata J, Lyne R, Burns G, Bahler J. 2002. The transcriptional program of meiosis and sporulation in fission yeast. Nat. Genet. 32:143–147. http://dx.doi.org/10.1038/ng951.
46. Voth WP, Yu Y, Takahata S, Kretschmann KL, Lieb JD, Parker RL, Milash B, Stillman DJ. 2007. Forkhead proteins control the outcome of transcription factor binding by antiactivation. EMBO J. 26:4324–4334. http://dx.doi.org/10.1038/sj.emboj.7601859.
47. Teytelman L, Thurtle DM, Rine J, van Oudenaarden A. 2013. Highly expressed loci are vulnerable to misleading ChIP localization of multiple unrelated proteins. Proc. Natl. Acad. Sci. U. S. A. 110:18602–18607. http://dx.doi.org/10.1073/pnas.1316064110.
48. Liang J, Lacroix L, Gamot A, Cuddapah S, Queille S, Lhoumaud P, Lepetit P, Martin PG, Vogelmann J, Court F, Hennion M, Micas G, Urbach S, Bouchez O, Nollmann M, Zhao K, Emberly E, Cuvier O. 2014. Chromatin immunoprecipitation indirect peaks highlight long-range interactions of insulator proteins and Pol II pausing. Mol. Cell 53:672–681. http://dx.doi.org/10.1016/j.molcel.2013.12.029.
49. Knott SR, Peace JM, Ostrow AZ, Gan Y, Rex AE, Viggiani CJ, Tavare S, Aparicio OM. 2012. Forkhead transcription factors establish origin timing and long-range clustering in *S. cerevisiae*. Cell 148:99–111. http://dx.doi.org/10.1016/j.cell.2011.12.012.
50. Chen HM, Rosebrock AP, Khan SR, Futcher B, Leatherwood JK. 2012. Repression of meiotic genes by antisense transcription and by Fkh2 transcription factor in *Schizosaccharomyces pombe*. PLoS One 7:e29917. http://dx.doi.org/10.1371/journal.pone.0029917.
51. Zaratiegui M, Castel SE, Irvine DV, Kloc A, Ren J, Li F, de Castro E, Marin L, Chang AY, Goto D, Cande WZ, Antequera F, Arcangioli B, Martienssen RA. 2011. RNAi promotes heterochromatic silencing through replication-coupled release of RNA Pol II. Nature 479:135–138. http://dx.doi.org/10.1038/nature10501.
52. Pebernard S, McDonald WH, Pavlova Y, Yates JR, III, Boddy MN. 2004. Nse1, Nse2, and a novel subunit of the Smc5-Smc6 complex, Nse3, play a crucial role in meiosis. Mol. Biol. Cell 15:4866–4876. http://dx.doi.org/10.1091/mbc.E04-05-0436.
53. Lee SY, Rozenzhak S, Russell P. 2013. gammaH2A-binding protein Brc1 affects centromere function in fission yeast. Mol. Cell. Biol. 33:1410–1416. http://dx.doi.org/10.1128/MCB.01654-12.
54. Heichinger C, Penkett CJ, Bahler J, Nurse P. 2006. Genome-wide characterization of fission yeast DNA replication origins. EMBO J. 25:5171–5179. http://dx.doi.org/10.1038/sj.emboj.7601390.